AD-A154 868 DOPPLER SATELLITE DATA CHARACTERISTICS(U) NAVAL SURFACE WEAPONS CENTER DAHLGREN VA R J ANDERLE OCT 83 NSWC/TR-83-353 1/1

UNCLASSIFIED F/G 20/14 NL

END

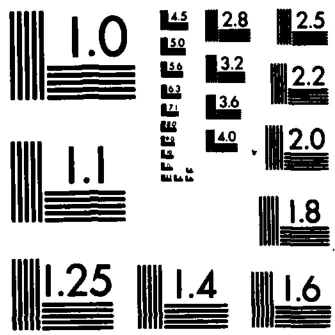

MICROCOPY RESOLUTION TEST CHART
NATIONAL BUREAU OF STANDARDS-1963-A

AD-A154 868

NSWC TR 83-353

DOPPLER SATELLITE DATA CHARACTERISTICS

BY R. J. ANDERLE

STRATEGIC SYSTEMS DEPARTMENT

OCTOBER 1983

Approved for public release, distribution unlimited.

NAVAL SURFACE WEAPONS CENTER

Dahlgren, Virginia 22448 • Silver Spring, Maryland 20910

	Copies
K05	30
K12	20
K13	20
K14	5

UNCLASSIFIED

SECURITY CLASSIFICATION OF THIS PAGE (When Data Entered)

REPORT DOCUMENTATION PAGE

READ INSTRUCTIONS BEFORE COMPLETING FORM

1. REPORT NUMBER: NSWC TR 83-353	2. GOVT ACCESSION NO.
3. RECIPIENT'S CATALOG NUMBER	
4. TITLE (and Subtitle): DOPPLER SATELLITE DATA CHARACTERISTICS	5. TYPE OF REPORT & PERIOD COVERED: Final
	6. PERFORMING ORG. REPORT NUMBER
7. AUTHOR(s): R. J. Anderle	8. CONTRACT OR GRANT NUMBER(s)
9. PERFORMING ORGANIZATION NAME AND ADDRESS: Naval Surface Weapons Center, Dahlgren, Virginia 22448	10. PROGRAM ELEMENT, PROJECT, TASK AREA & WORK UNIT NUMBERS: NIF
11. CONTROLLING OFFICE NAME AND ADDRESS: Defense Mapping Agency Headquarters, Washington, D. C. 20305	12. REPORT DATE: October 1983
	13. NUMBER OF PAGES: 56
14. MONITORING AGENCY NAME & ADDRESS (if different from Controlling Office)	15. SECURITY CLASS. (of this report): UNCLASSIFIED
	15a. DECLASSIFICATION/DOWNGRADING SCHEDULE

16. DISTRIBUTION STATEMENT (of this Report)

Approved for public release; distribution unlimited.

17. DISTRIBUTION STATEMENT (of the abstract entered in Block 20, if different from Report)

18. SUPPLEMENTARY NOTES

19. KEY WORDS (Continue on reverse side if necessary and identify by block number)

Doppler
Navigation
Geodesy

Accession For	
NTIS GRA&I	X
DTIC TAB	☐
Unannounced	☐
Justification	
By	
Distribution/	
Availability Codes	
Dist	Avail and/or Special
A/,	

DTIC COPY INSPECTED 3

20. ABSTRACT (Continue on reverse side if necessary and identify by block number)

Random, oscillator and ionospheric errors are reviewed for Doppler observations of satellites. For omnidirectional antennas, random errors of Doppler measurements over 30-second intervals exceeded 20 cm about 30 percent of the time yielding measurement precision in the satellite position of about 50 cm based on a pass of data. High gain antennas showed random errors of only a few centimeters, but gave a precision in position of only 4 m because of the short Doppler count normally made with the equipment

DD FORM 1 JAN 73 1473 EDITION OF 1 NOV 65 IS OBSOLETE

S/N 0102-LF-014-6601

UNCLASSIFIED

SECURITY CLASSIFICATION OF THIS PAGE (When Data Entered)

considered. However, oscillator errors significantly degrade this precision unless stabilities of about 5X10^{-13} are achieved for averaging times of about 1000 seconds. If such oscillators are utilized, a higher precision in position determination can be realized for continuously counted Doppler data by exploiting the continuous character of the measurement in the processing of the data.

Neglected higher order ionospheric effects produce measurement errors equivalent to a meter or more during periods of high solar activity.

FOREWORD

Doppler satellite observations have been used for geodetic applications since 1960. Until recently, uncertainties in atmospheric drag and in knowledge of the earth's gravity field have been the principal limitations to the accuracy of the system. Now with improved determinations of the gravity field, drag compensation on some satellites and higher altitudes of other satellites, instrument errors are assuming more importance. This report compares random instrument errors for different satellites and receivers, examines systematic errors due to oscillators and neglected higher order ionospheric effects, and discusses various methods of interpreting the data.

Released by:

Thomas A. Clare

THOMAS A. CLARE, Head
Strategic Systems Department

CONTENTS

ILLUSTRATIONS

INTRODUCTION

Doppler satellite observations of Navy Navigation Satellites have been used since 1963 to determine the positions of sites in an earth-centered geodetic coordinate system. The positions of the receivers were computed on the basis of precise ephemerides computed by the Naval Surface Weapons Center until 1972, at which time the Defense Mapping Agency Hydrographic Topographic Center assumed responsibility for the computations. The methods of computation of the satellite ephemeris were changed periodically to obtain improved accuracy until 1972, at which time positions were computed to an accuracy of about a meter. Since that time, relatively small changes were made in the computational procedures or in the accuracy, although a better understanding was obtained of systematic errors (Leroy, 1982). A review of the error sources is given by the author (Anderle, 1976).

Two of the principal error sources affecting computed geocentric coordinates of observing sites are the effects of uncertainties in knowledge of the gravity field and atmospheric drag forces on the motion of the satellite. However, there are circumstances under which these are not dominant error sources: 1. When positions of sites observing the same satellite passes are computed, errors in the satellite orbit are common and their effects on computed relative position of the sites can be reduced; 2. The "NOVA" Navy Navigation Satellite is equipped with sensors and thrusters to compensate for the principal effects of variations in atmospheric drag and solar radiation; 3. Computed orbits of satellites at higher altitudes than the Navy Navigation Satellites, such as the proposed TOPEX altimetry satellite (anon., 1982), are less subject to uncertainties in the earth's gravity field and atmospheric drag. These factors, coupled with the effects of increased solar radiation in recent years on measurement accuracy and changes in satellite and ground equipment made it desirable to reexamine instrument accuracy. This report considers the effects of random oscillator and ionospheric correction errors on instrument performance, and discusses the interpretation of the Doppler measurements with respect to the determination of satellite or station positions.

INSTRUMENTATION

Two important contributors to the accuracy of Doppler measurements are the stabilities of the oscillators in the spacecraft and the ground. Oscillator errors contribute to uncertainties both in the time-tagging of the observations and in the Doppler measurement, but the latter is the critical limiting factor.

Doppler measurements are made at 1- to 30-second intervals, depending on the type of receiver, for the 1000-second time interval that the satellite is in view. Oscillator instabilities over the measurement interval are detected in preprocessing programs and interpreted as random errors of observations while instabilities over periods approaching the length of the pass cause systematic errors which cannot be distinguished from orbit errors. Crystal oscillators have been used in all spacecraft discussed in this report while receivers discussed are variously equipped with crystal, Rubidium or Cesium oscillators. The "OSCAR" type Navy Navigation satellites have crystal oscillators procured in the 1960's which have a stability of $5X10^{-11}$ at a 30-second averaging time while the "NOVA" type Navy Navigation satellite launched in 1981 has a stability of $5X10^{-12}$ over 30 seconds (Hoskins, 1982). The SEASAT altimetric satellite, launched in 1978 and also discussed in this report, probably had stability intermediate between these two. Values of the stability for averaging times near 1000 seconds are not available in the literature, but typically degrade for crystal oscillators.

Three classes of receivers are discussed in this report: (1) "OPNET" receivers used at the four sites in the operational Navy Navigation Satellite System; (2) "TRANET" receivers used at semi-permanent sites managed by, or cooperating with, the Defense Mapping Agency; and (3) portable receivers (GEOCEIVERS or MAGNAVOX MX-1502) deployed periodically by the Defense Mapping Agency. The OPNET sites usually employ high gain tracking antennas, make Doppler measurements starting every four seconds over a time interval a little less than a second, and use Cesium oscillators. All other receivers discussed in this report employ omnidirectional antennas and read out continuously counted Doppler measurements at intervals in the neighborhood of 30 seconds. The TRANET sites were originally operated from crystal oscillators except that the cooperating stations in Uccle, Misawa, and Florence have utilized Cesium or Rubidium oscillators since their initial operation. Seychelles was converted to Cesium in February 1979 and the other sites were equipped with Rubidium oscillators on the following schedule: October 1969 for New Mexico; April 1974 for Brazil, Alaska, South Africa, Thule; June 1974 for the Philippines; July 1974 for Australia; 1978 for Ottawa; July 1979 for Herndon; August 1979 for England; September 1980 for Guam and Samoa; May 1982 for McMurdo; and February 1983 for Austin. Calgary is still operating on a Quartz. The TRANET-1 equipment, which was constructed in the late 1950's and early 1960's, was converted from sample Doppler to continuous count Doppler in 1971 and early 1972, and began to be replaced by modern electronics (TRANET 2) starting in 1979. The portable equipment used periodically for ephemeris calculations was GEOCEIVERS until 1982, at which time MAGNAVOX MX-1502 receivers were deployed. Crystal oscillators were utilized with the equipment until mid-1982, at which time Efratom Rubidium oscillators were installed. The Rubidiums were repackaged for better temperature control in early 1983.

RANDOM ERROR OF OBSERVATION

During preprocessing of Doppler data, residuals are obtained with respect to a nominal orbit, systematic trends are removed, and the trend-free residuals are rms'd to obtain an estimate of the random error of observation which is

used to compute a weight for the data in the orbit computation. Sample results of such computations are given in Appendix A, Figures A-1a--A-1g as distribution functions, in Figures A-2a--A-2g for each station, and in Figures A-3a--A-3f versus elevation angle. The rms of the residuals is given in cm in all cases. The cases given are:

Figure a - Sat 77 (NAVSAT OSCAR. 1973-81A) 1978
b - Sat 98 (SEASAT, 1978-64A) 1978
c - Sat 68 (NAVSAT OSCAR, 1970-67A) 1982
d - NOVA (NAVSAT, 1981-44A) 1982
e - Sat 68 (NAVSAT OSCAR) 1983 Doppler data
f - Sat 68 (NAVSAT OSCAR) 1983 Range data
g - Sat 68 (NAVSAT OSCAR) 1983 Doppler data normal processing.

Systematic trends were removed by special processing in generating Figures a-f, while Figure g was obtained from normal preprocessing which should be more effective. Figures a-e were generated to test the effects of different satellite oscillators, different ionospheric levels and TRANET 1 upgrade effects. However, it appears such effects are masked by variations in performance of individual stations. For Figure f, Doppler data were accumulated during the pass to form a stronger data class, biased range, rather than range difference. Residuals should be larger for the range data class because of oscillator effects, but again the effect is not noticeable in the results. The normal processing, Figure g, was produced to ensure that the filtering and trend removal for the earlier figures was as effective as normal processing. Figure g versus e shows the programs give reasonably similar results.

Figures A-1 show that about 30 percent of the passes have random errors exceeding 20 cm. One point of interest is the extremely small random error for the OPNET stations which utilize directional antennas.

TRANSFORMATION FROM DOPPLER ERROR TO POSITION ERROR

Errors in Doppler measurements cannot be directly transformed into errors in computed station positions or computed satellite positions. It has been customary to assume, for diagnostic purposes, that a pass of Doppler data over a station determines the range from the station to satellite and the along track (tangential) relative position of the station and satellite, along with frequency and refraction biases. Actually, the third position component and the velocity components are coupled to some extent with the two position components normally computed for diagnostic purposes. Table 1 shows the first four of six eigenvalues and corresponding eigenvectors for six sample passes. In representing the relative importance of position and velocity, velocity components in the normal equations were multiplied by a factor of 1000. This factor is reasonable from either of two points of view: (1) the pass is about 1000 seconds long, and (2) comparisons of orbits for different gravity fields show position differences in km about 1000 times the velocity differences in km/sec.

Table 1 shows the first two eigenvalues are two or three orders of magnitude greater than the third eigenvalue, and the third eigenvalue is one or two orders of magnitude larger than the fourth (the fifth and sixth are one or two orders

TABLE 1. SAMPLE EIGENVALUES AND EIGENVECTORS

		Eigenvector Components					
		Position			Velocity		
Zenith Angle	Eigenvalue	Radial	Tangential	Transverse	Radial	Tangential	Transverse
69°	.17E07	.71	.44	.08	.16	-.51	.04
	.11E07	.38	-.83	.04	-.30	-.27	-.07
	.13E04	.58	.00	-.16	-.01	.80	-.04
	.43E02	-.02	.19	.03	-.30	-.03	-.93
40°	.98E07	.61	.73	-.04	.16	-.25	-.03
	.35E07	.64	-.64	-.06	-.14	-.40	.02
	.16E05	.47	-.07	.14	-.04	.87	.02
	.14E04	.01	-.19	-.02	.73	.03	-.66
24°	.96E07	.81	-.45	.03	-.09	-.37	-.01
	.36E07	.40	.87	.02	.18	-.23	.01
	.43E05	.44	.03	-.09	.04	.89	.01
	.49E03	-.01	-.19	.05	.88	-.03	.43
17°	.70E07	.81	.41	-.03	.09	-.41	-.01
	.40E07	.36	-.89	-.01	-.20	-.21	.01
	.56E05	.46	-.01	.07	-.05	.89	.02
	.11E04	-.02	.21	-.01	-.92	-.05	.31
50°	.12E08	.85	.13	-.08	.04	-.51	-.01
	.60E07	.12	-.95	-.01	-.27	-.08	.05
	.38E05	.52	.00	.15	.00	.84	-.01
	.57E03	-.01	-.21	.00	.59	.00	-.78
39°	.11E08	.03	.97	.00	.24	-.01	-.03
	.64E07	.88	-.03	-.06	.00	-.47	.00
	.28E05	.47	.01	.13	-.03	.87	.02
	.17E04	.01	-.21	-.01	.74	.04	-.64

still smaller). However, although the first two eigenvalues are largely in the range and tangential direction, there are significant components along a velocity component. For normal navigation purposes, the correlation with velocity is of no concern since ship position error is so much larger than the equivalent relative velocity error. But for ephemeris determination, standard errors computed for two components of position may yield an overly optimistic view of the value of Doppler data because of the effect of satellite velocity errors.

Even discounting the effects of uncertainties in the relative velocity of the satellite and receiver, the representation of the information content of a Doppler pass by the tangential and radial errors is imperfect. If these two components were principal eigenvalues of the position solution, then loose a-priori on a three-component solution should yield the same solution as a constrained solution. Figures A-4 show that this is not the case. Although a loosely constrained three-parameter solution yields the same solution for the tangential component of position as does the two-parameter solution (Figure A-4a), the three-parameter solution for range (or radial) error only agrees with a two-parameter solution for an appropriate a-priori for the position components (Figure A-4b). (Two and three parameters refer to the number of position component parameters; frequency and refraction bias were parameters in all cases.) Figures A-4 were generated for a reference frame defined in earth-fixed space; it is not known whether the coupling of the range and out-of-plan components exists only in this space or also in inertial space, in which the eigenvalues and eigenvectors of Table 1 were generated. Note in Table 1 that the radial eigenvector has significant components for the first three eigenvalues.

SATELLITE POSITION ERRORS VS RECEIVER TYPE

Despite the reservations expressed in the preceding section, studies were conducted of the uncertainties in radial and tangential position of the satellite as a function of data class. Figures A-5a--A-5c give (a) the rms errors, (b) the root weighted square (rws) errors, and (c) the standard errors in the range component of the position of the satellite as a function of elevation angle at closest approach for various types of receiver equipment. (The tangential component of p[illegible]n errors are fairly similar.) Figures A-5a and A-5b reflect both epheme[illegible]d equipment errors, where the ephemeris errors dominate generally. Figure A-5c gi[illegible] only the effects of random error of observation as defined by Figures A-1-[illegible]3. Figure A-4a, the root mean square error for observations above 5° eleva[illegible]n angle and passes exceeding 10° elevation angle, gives the overall syste performance considering both ephemeris and observation errors. Different tol rances for elevation angle would radically alter this curve. Figure A-4b, the root weighted square range errors, represents the best estimate of the actual ephemeris errors since weak observations are deweighted. The curves indicate the ephemeris error is about 1 m. On the other hand, the weighting tends to give not the typical, but rather the best, performance of the Doppler receivers with the current dynamic model. Figure A-5c, the standard error in range (or radial) position of the satellite, gives the precision in position determination corresponding only to the inferred random error of observation, discounting gravity and other dynamic errors and most of the oscillator error. These curves are not markedly different for the different types of receivers

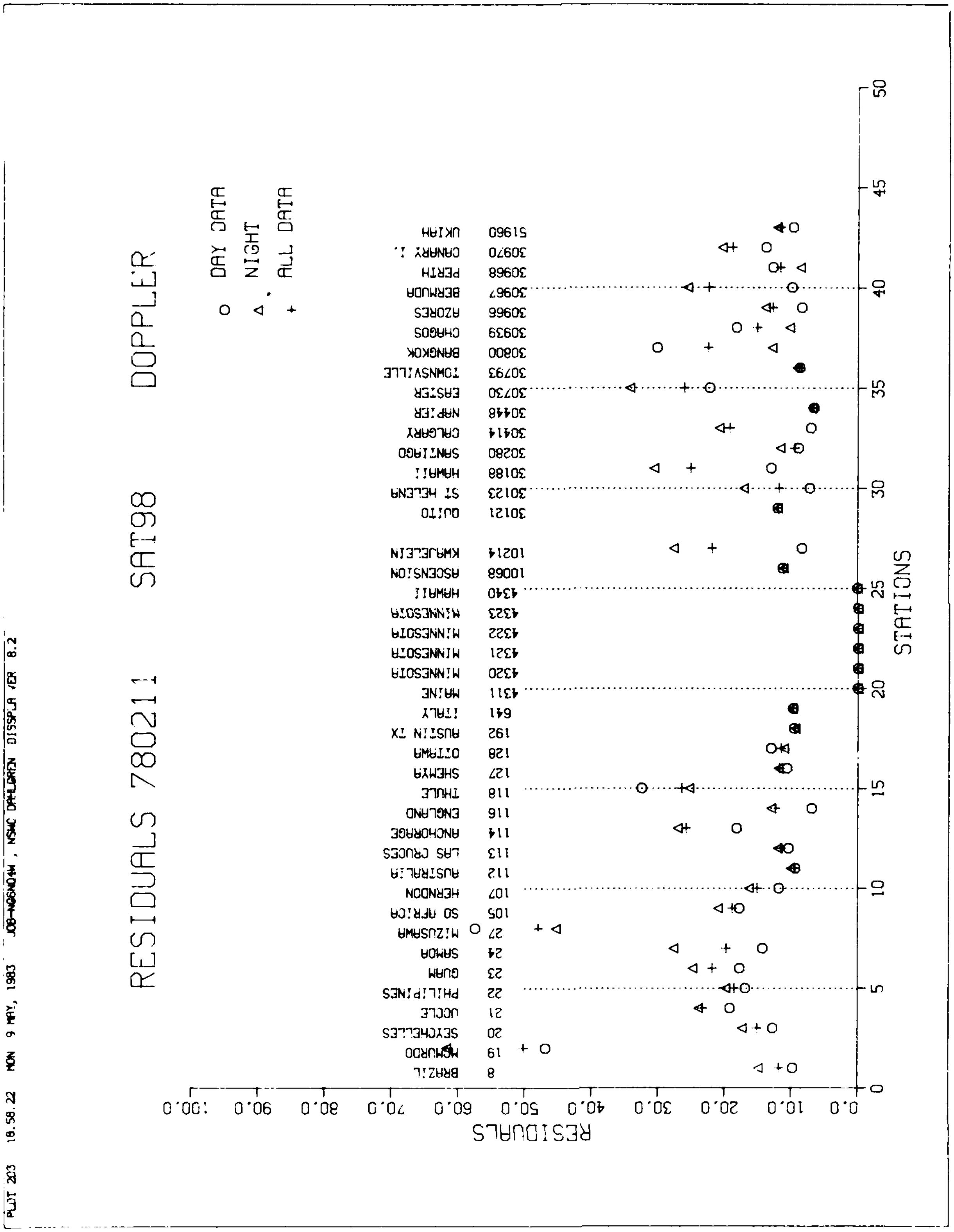

FIGURE A-2b. RESIDUALS BY STATION, SATELLITE 98, 1978

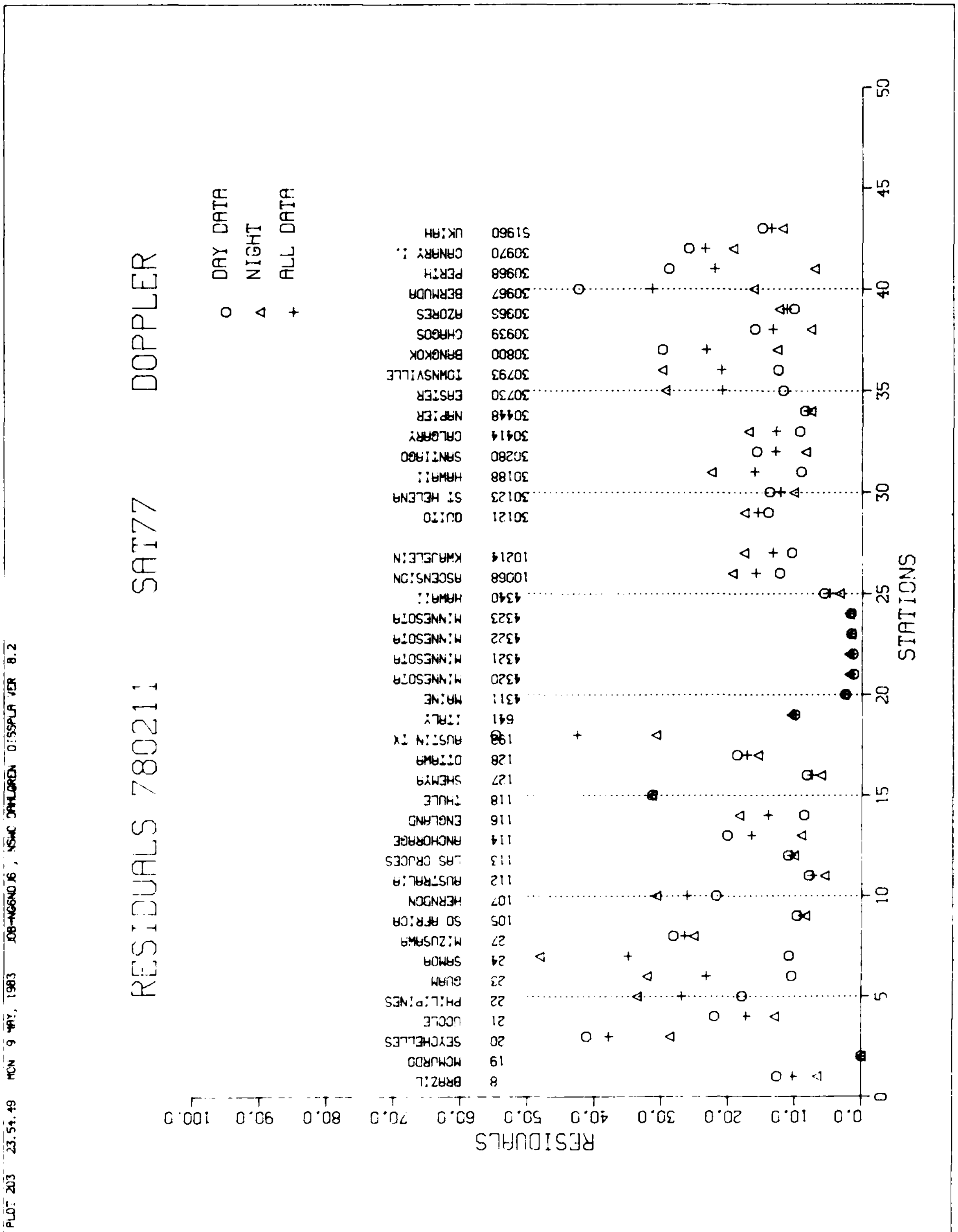

FIGURE A-2a. RESIDUALS BY STATION, SATELLITE 77, 1978

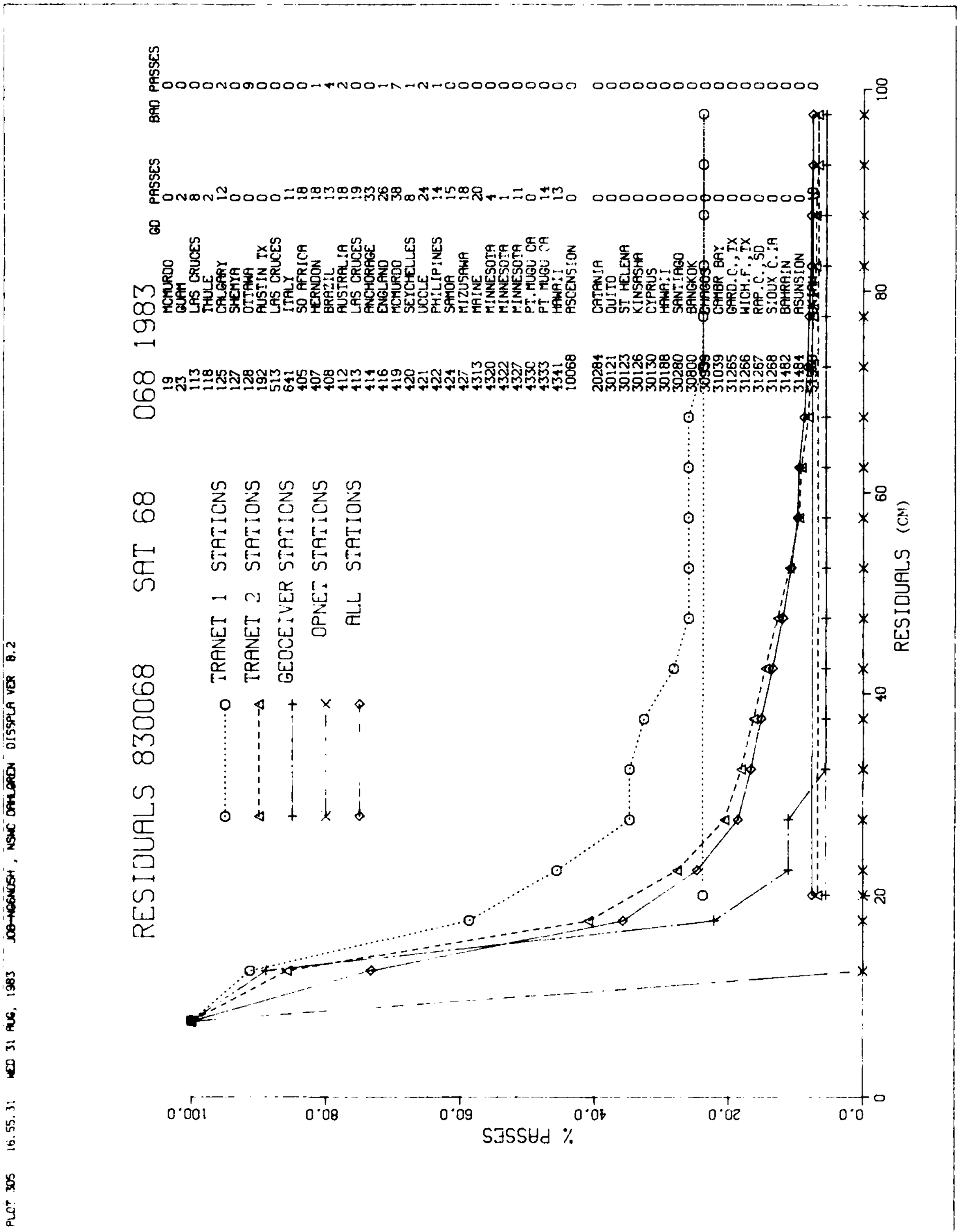

FIGURE A-1g. DISTRIBUTION OF RESIDUALS, SATELLITE 68, 1983, NORMAL PROCESSING

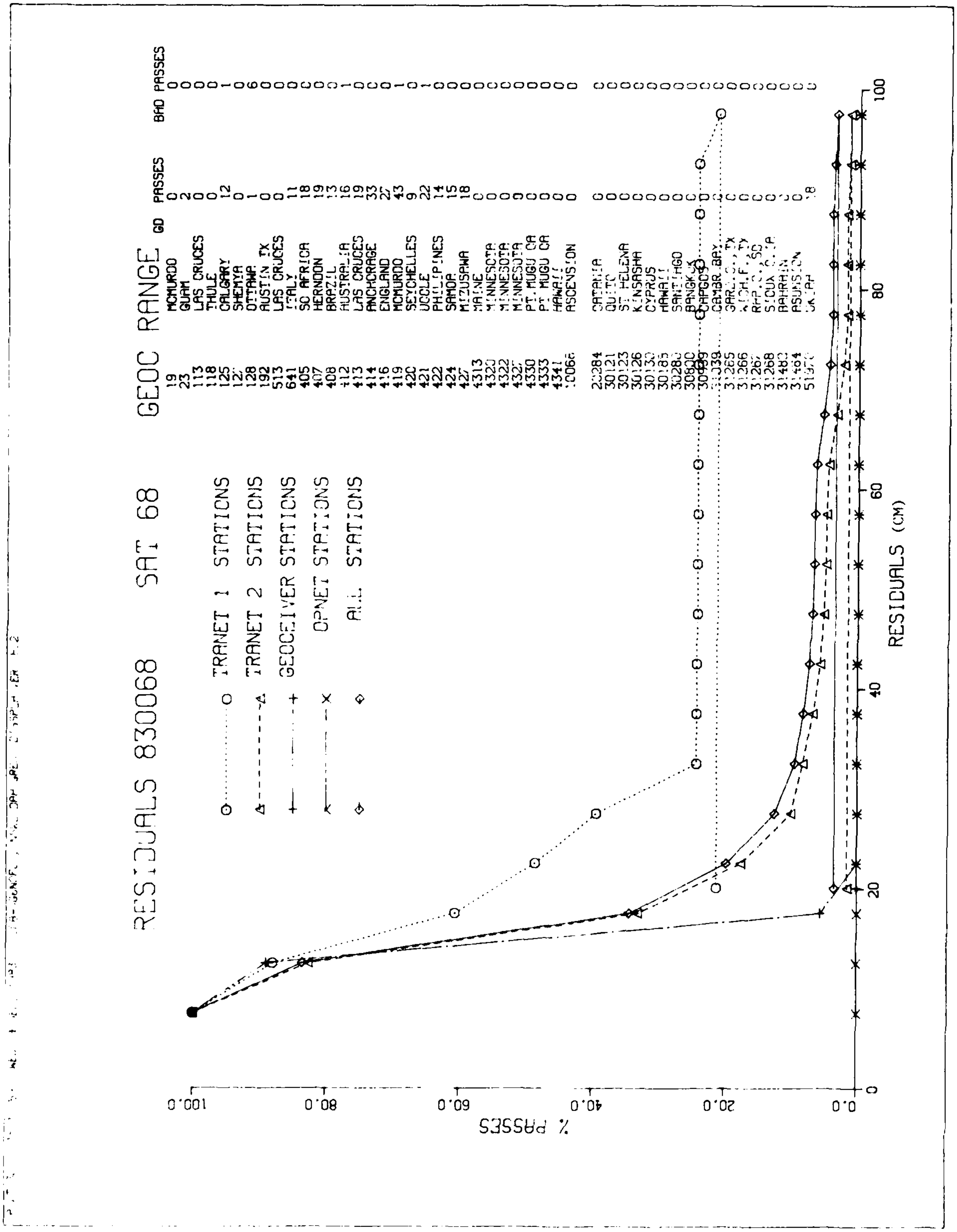

FIGURE A-1f. DISTRIBUTION OF RESIDUALS, SATELLITE 68, 1983, RANGE DATA

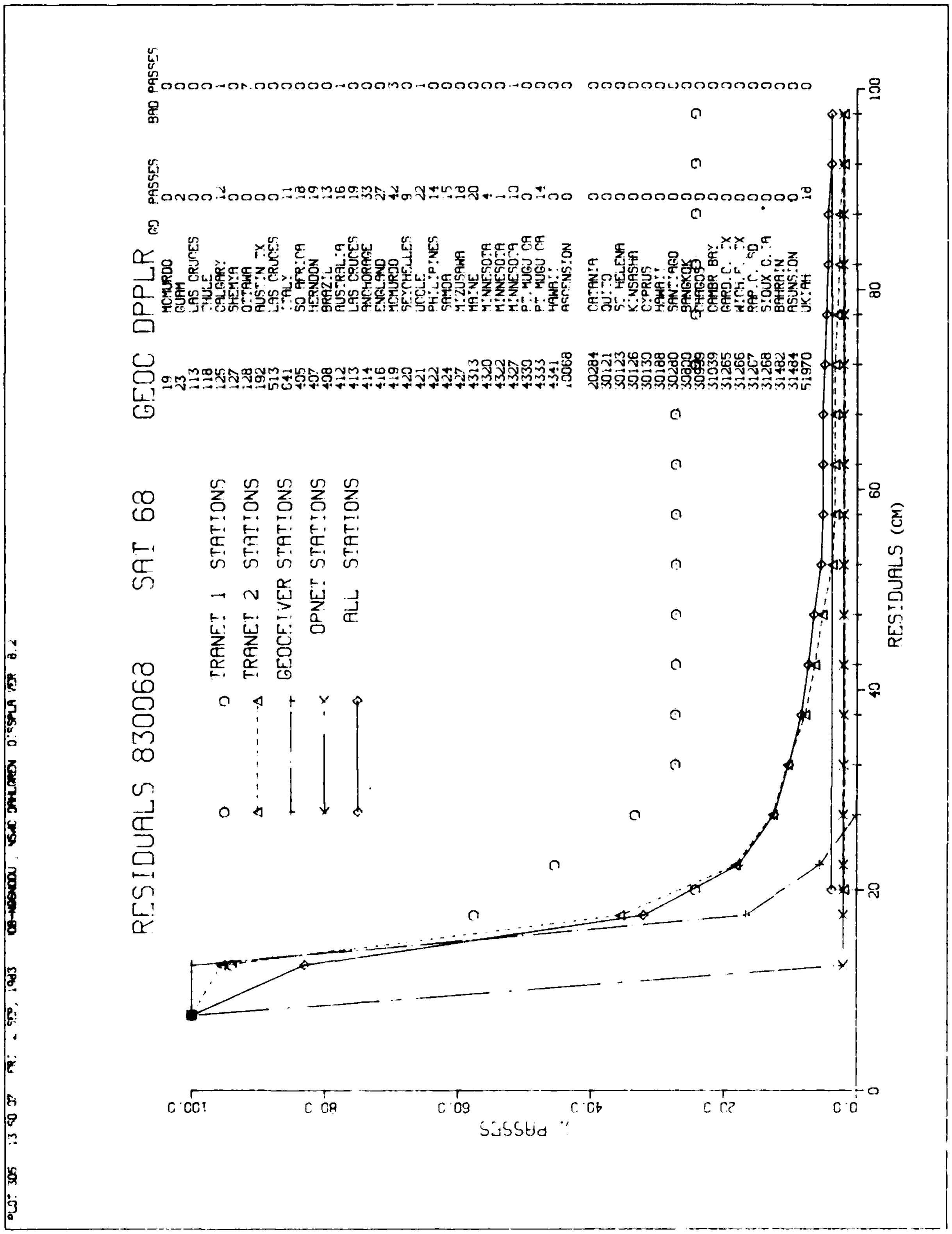

FIGURE A-1e. DISTRIBUTION OF RESIDUALS, SATELLITE 68, 1983

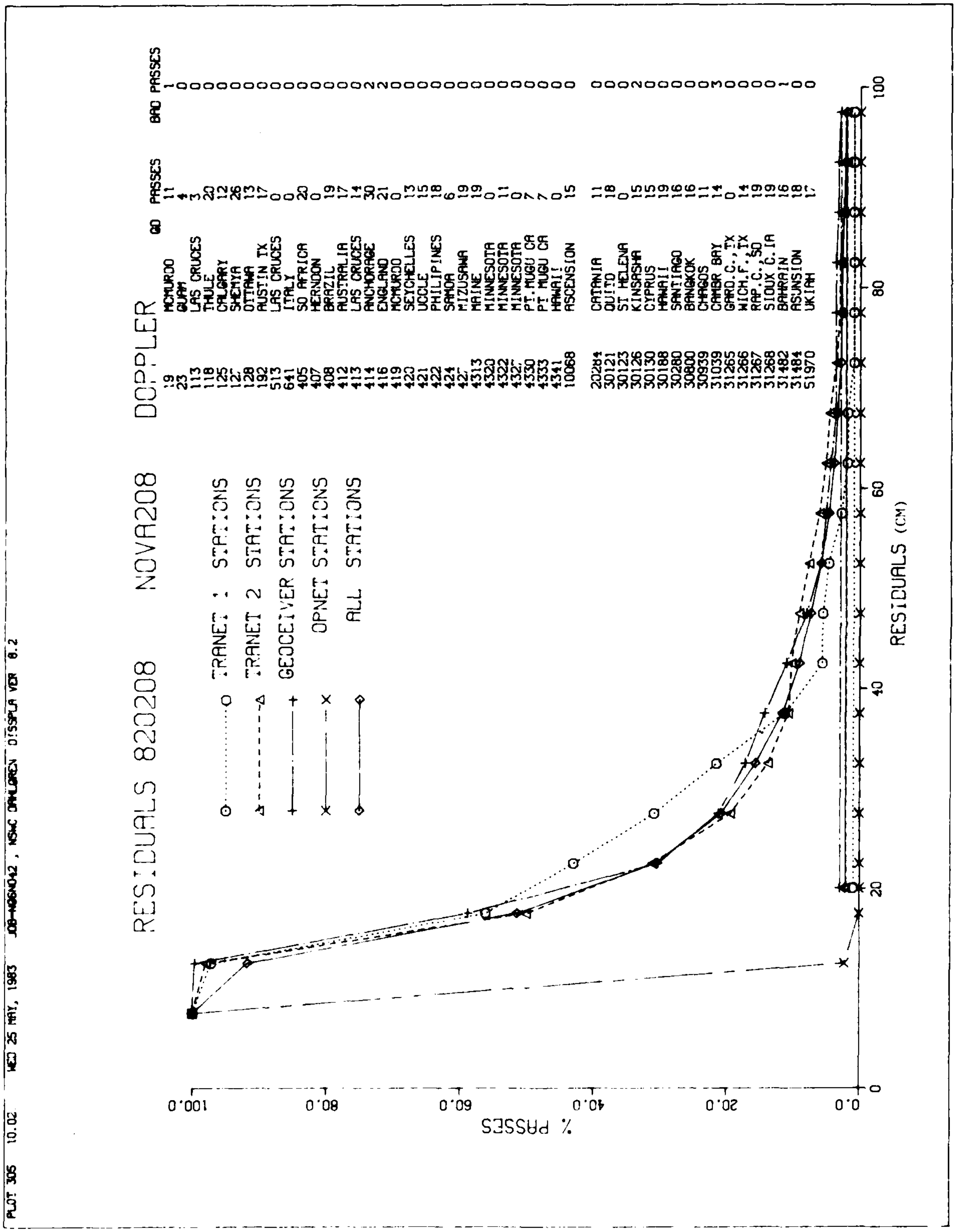

FIGURE A-1d. DISTRIBUTION OF RESIDUALS, NOVA, 1982

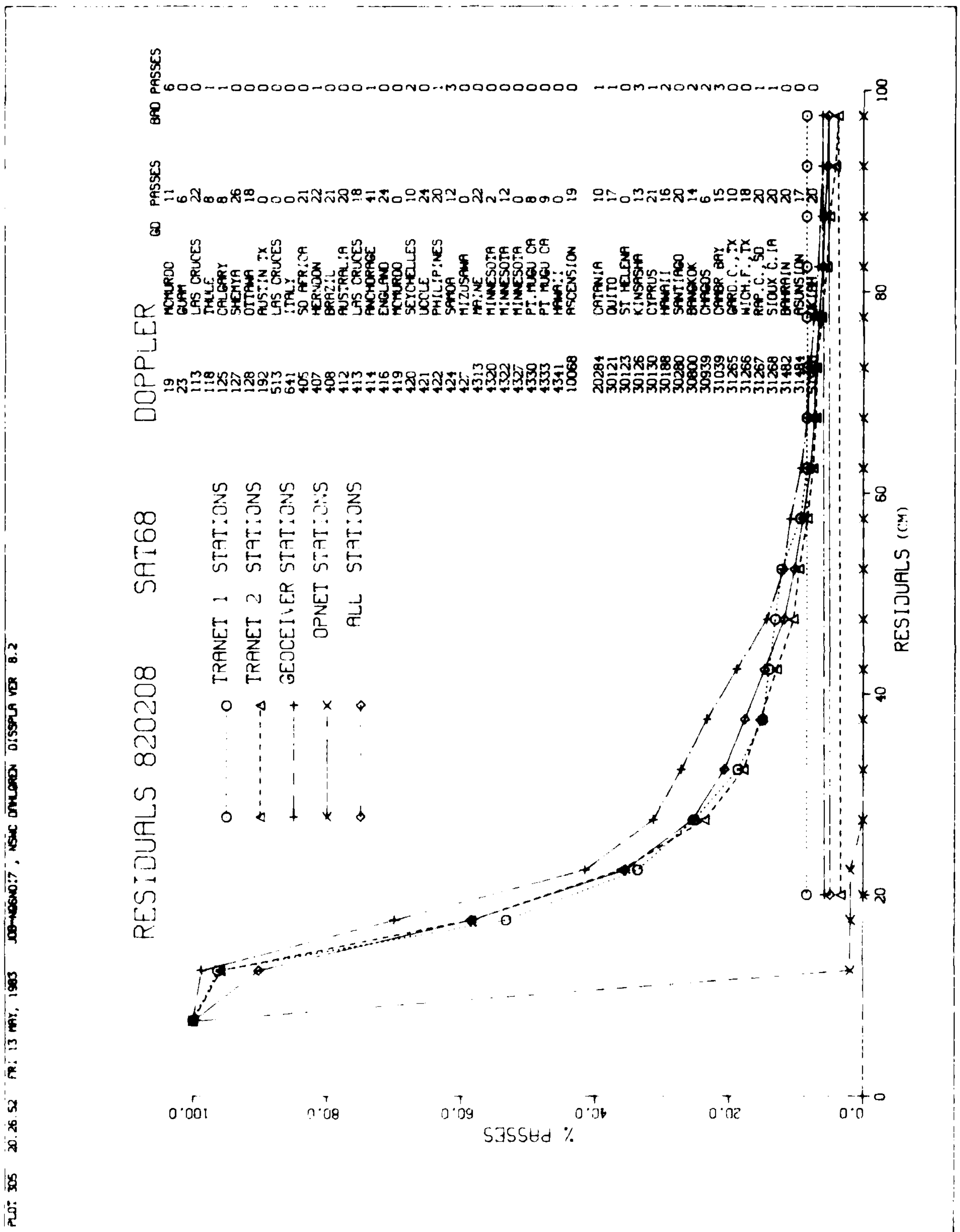

FIGURE A-1c. DISTRIBUTION OF RESIDUALS, SATELLITE 68, 1982

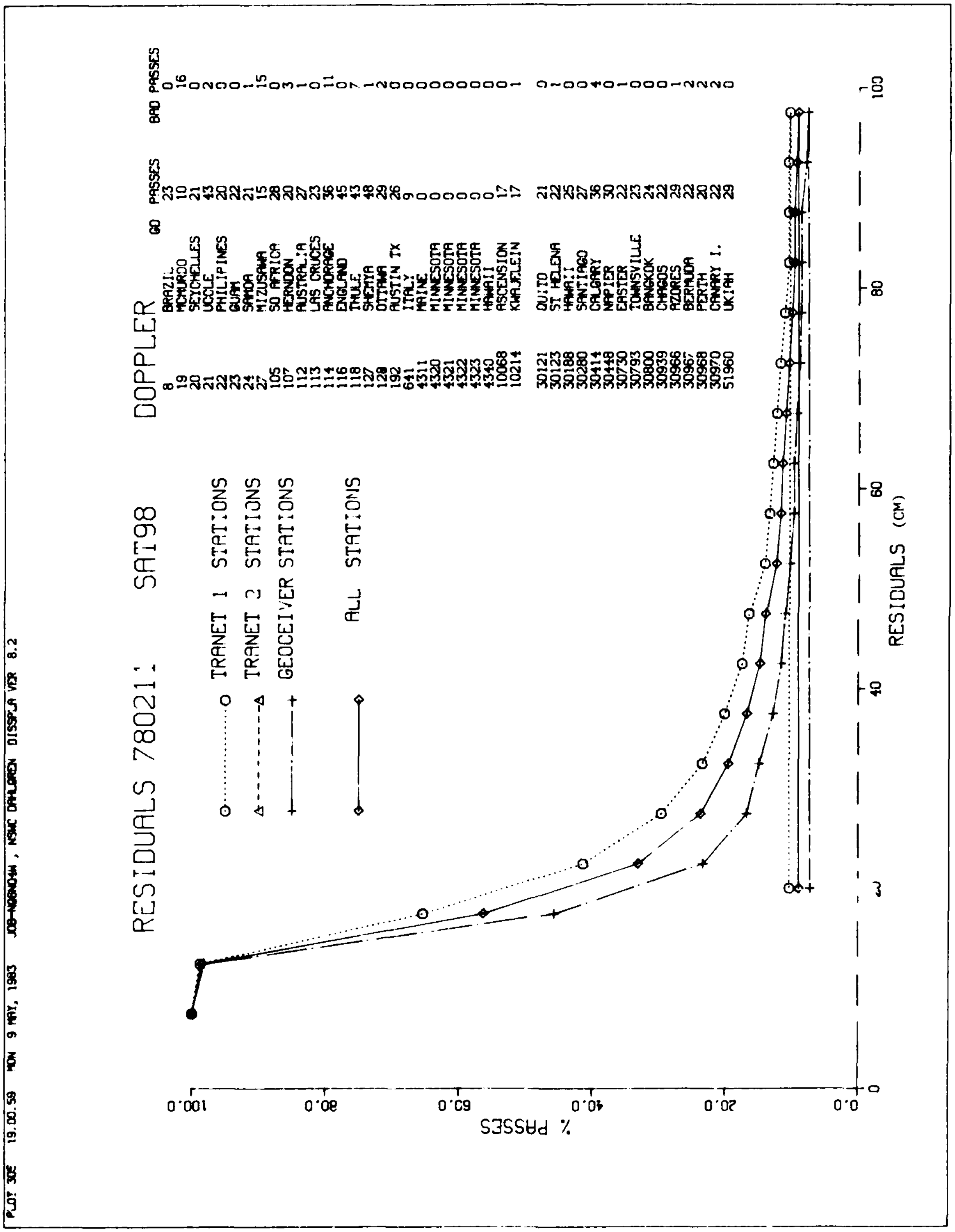

FIGURE A-1b. DISTRIBUTION OF RESIDUALS, SATELLITE 98, 1978

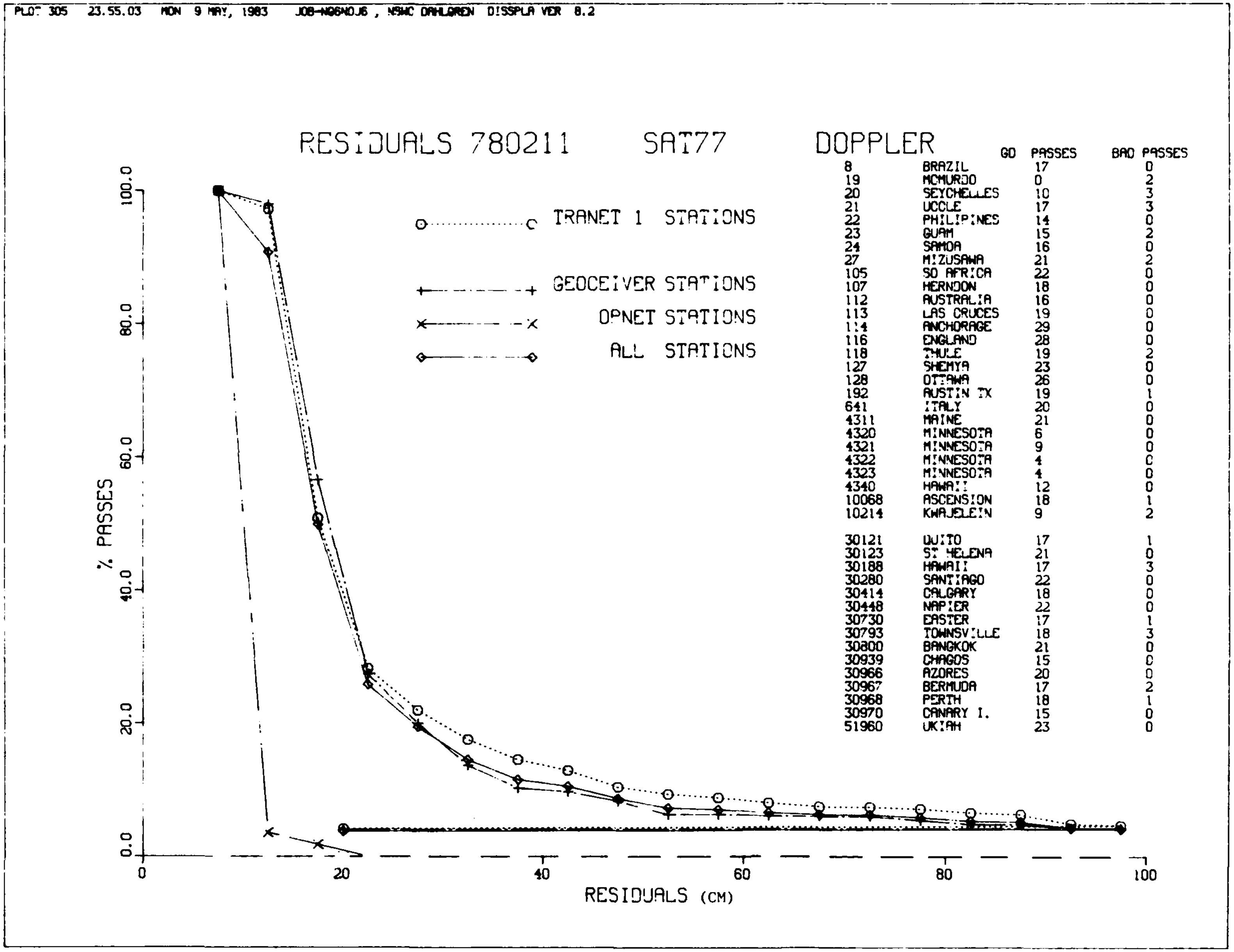

FIGURE A-1a. DISTRIBUTION OF RESIDUALS, SATELLITE 77, 1978

APPENDIX A

FIGURES

BIBLIOGRAPHY

__________, "Ocean Topography Experiment (TOPEX) Mission Description," Jet Propulsion Laboratory Report JPL D-601, December 1982.

Anderle, R. J., "Error Model for Geodetic Positions Derived from Doppler Satellite Observations," *Bulletin Geodesique* 50(1), pp. 43-77, 1976.

Clynch, James R. and Brent A. Renfro, "Evaluation of Ionospheric Residual Range Error Model," *Proceedings of the Third International Symposium on Satellite Doppler Positioning*, Physical Science Laboratory, New Mexico State University, pp. 517-537, 1982.

Gouldman, M. Wendel Spence, "Oscillator Studies," *ibid.*, pp. 67-69.

Hoskins, Gerald W., "Navy Navigation Satellite System Status," *ibid.*, pp. 825-841.

Leroy, Caroline F., "The Impact of GRS-80 on DMA Products," *ibid.*, pp. 129-150.

HIGHER ORDER IONOSPHERIC EFFECTS

There are long and short period variations in solar activity as shown in Figure A-9 (the lower two curves refer to the orientation of the orbit of one or another NAVSAT satellites relative to sun). Although first order ionospheric effects are removed from the observational data by appropriate combination of measurements made on two coherent frequencies emitted by the satellite, neglected higher order ionospheric effects can be significant during periods of high solar activity, such as those experienced in recent years. Clynch and Renfro (1982) developed a simple algorithm for computing the higher order effects on the basis of the first order effect. Figure A-10 shows the effects of solar activity on computed station position due to simulated third order ionospheric effects for a number of geographic positions, for two levels of solar activity, and a particular orientation of the orbit plane relative to the sun. The effects can be radically different for other sun-orbit orientations. Figure A-11 shows the dependence of the computed height of the station on solar flux index for stations at various geographic locations; the effects significantly exceed 1 m for a solar flux index of 200 for stations near the geomagnetic equator. Effects on computed orbit positions can be expected to be comparable. The dependence of computed height on critical frequency as inferred from actual observations is given in Figure A-12, which is taken from an NSWC IUGG report on plate motions.

c. Range to satellite error for given proportional frequency error (Figure A-8). This figure, drawn from the results of Monte Carlo simulations reported by Gouldman (1982), indicates that a proportional frequency error of $5X10^{-13}$ is required to provide 10 cm NAVSAT or TOPEX range and tangential errors (i.e. a net $5X10^{-13}$ between satellite and station oscillators).

d. Since normal (excluding BVA resonant) crystal oscillators do not achieve $5X10^{-13}$ stability, Rubidium oscillators have been installed in ground receivers. These oscillators have the characteristic of a $\sqrt{t}$ reduction in oscillator stability to a flicker floor. A simulation is planned for completion by 1 January 1984 to determine the effect of different flicker floors reached at a 1000-second averaging time on position accuracy.

The shaded area of Figure A-7 is proposed as specification limits for Doppler oscillators. Integrated errors less than 1 cm are negligible compared to phase measurement errors for omnidirectional antennas (10 percent at a wavelength of 75 cm), while errors exceeding 10 cm are beginning to significantly degrade instrument performance, particularly at the longer averaging time. Note that the measured performance of two sample quartz oscillators (which is significantly better than specifications) is adequate at the shorter averaging time, but badly out of the proposed standard at the longer averaging time. The specification for the Efratom Rubidium oscillator fits nicely in the envelope for the proposed standard, but many of the oscillators tested failed to meet the specifications even in a laboratory; the bounds for the measurements for a dozen or so Rubidium oscillators are indicated in Figure A-7 by the legend "R_b measured." Measurements have not been made at the longer averaging times because of the longer time required to make the tests and the press of operational commitments. Neither have measurements been made on the atomic oscillators at the TRANET sites. However, the HP 5065 R_b oscillators have performance specifications similar to the Efratom R_b, while Cesium standards are normally worse at all averaging times of interest for Doppler measurements.

The differences among the various curves in Figure A-8 are probably not statistically significant since each point is the root mean square of only six measurement errors. The curve indicates a relative frequency stability of $5X10^{-13}$ is required to achieve 10 cm precision in the computed position of the satellite relative to the station. Since two oscillators (satellite and receiver) are involved, the specification should be divided by $\sqrt{2}$ for each oscillator, or perhaps more due to possible aliasing of velocity and position errors. On the other hand, the error was computed for an oscillator with a constant fractional frequency stability, such as might be possible for a crystal oscillator. Further tests will probably show that the specification of the flicker floor for a Rubidium oscillator can be higher.

except for the OPNET receivers. The OPNET receivers, which had the lowest random error in range difference in Figures A-1--A-3 due to their high gain antennas, have the poorest standard error of observation of range to the satellite (Figure A-5c) due to the short data measurement interval. The OPNET receivers count range difference at 4-second intervals over time spans less than 1 second while the GEOCEIVERS count over contiguous 30-second intervals. Although there are five or six times as many OPNET observations in a 20- or 30-second TRANET or GEOCEIVER observation interval, which increases the OPNET precision of position determination by the square root of five or six, the information content relative to the random error is directly proportional to the observational interval which is 20 or 30 times greater for TRANET or GEOCEIVER relative to OPNET receivers. The net effect is that, due to their longer count intervals, the TRANET and GEOCEIVERS give better precision in position determination (about 50 cm for above 30° elevation) than the higher data rates and higher precision (antenna gain) of the OPNET receivers. The fact that Figures A-5a and A-5b show little difference between receiver types simply means that dynamic (mostly gravity) errors dominate random instrument errors in NAVSAT calculations.

SATELLITE POSITION ERRORS VERSUS DATA REPRESENTATION

Although most (excluding OPNET) Doppler receivers make continuous counts of Doppler data, most computing centers consider each Doppler count to be independent of the neighboring count. This illogical assumption is justified by the quality of the satellite and receiver oscillators in current use, as discussed in the next section. Figures A-6a--A-6b compare actual rms and rws range errors for the two representations of data while Figure A-6c indicates the range orbit errors to be expected for the two representations of data if oscillator errors were not a consideration. The fact that the rms and rws errors for range are somewhat higher than those for Doppler data in Figures A-6a and A-6b may be due to either the difference in number of passes processed with the two data types or due to relatively naive computational techniques employed in converting range difference to range data class. Figure A-6c indicates the strength of solution for the range bias data class is about a factor of two better than the strength of solution for a range difference data class, when oscillator stability is not a consideration.

OSCILLATOR STABILITY

The effect of oscillator stability on the accuracy of Doppler data can be approximated in various ways:

a. Range difference error = proportional frequency error X speed of light X count interval (Figure A-7).

b. Range difference error over a given time for a given proportional frequency error; Fell (private communication) has shown these errors to be not much smaller than method a.

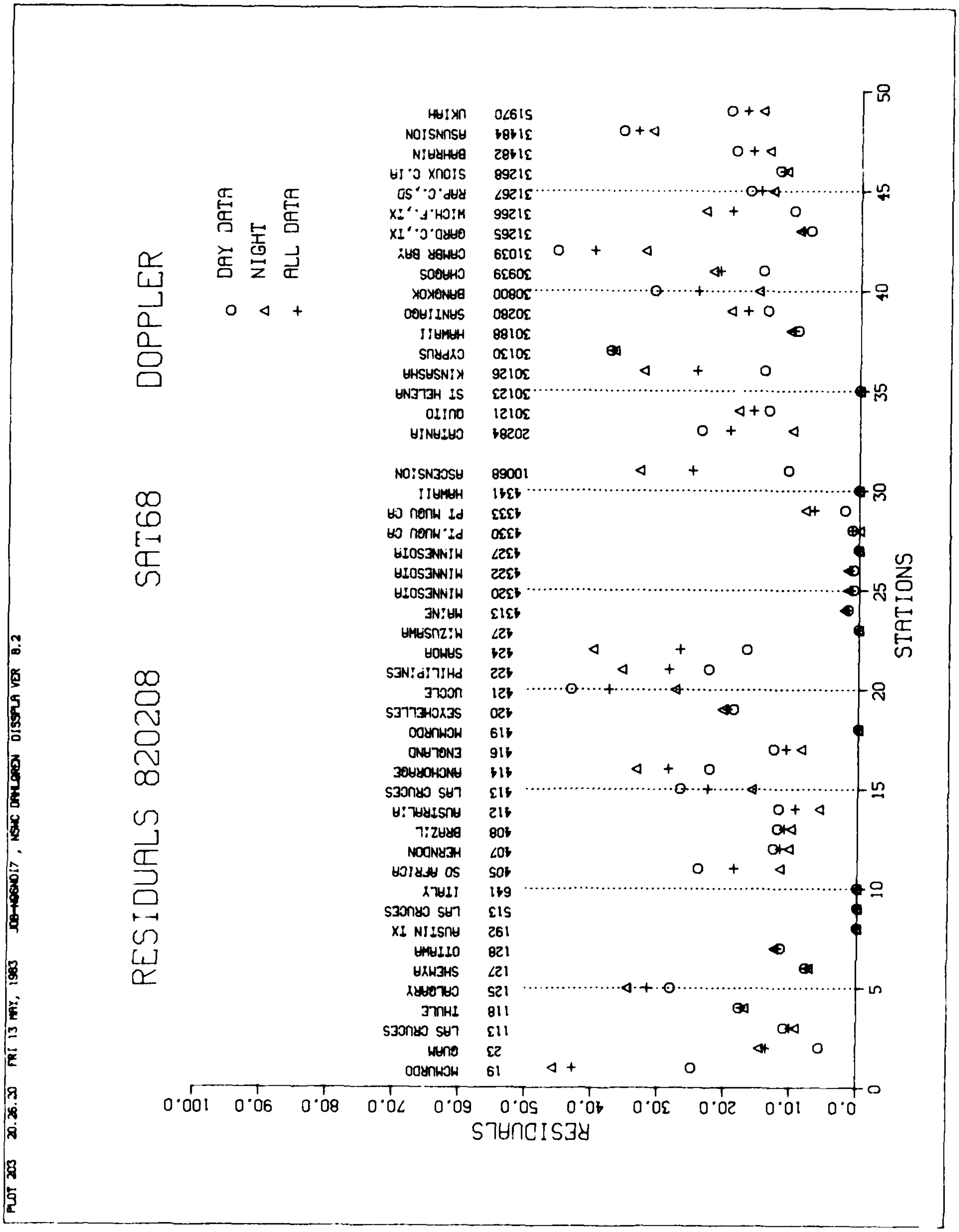

FIGURE A-2c. RESIDUALS BY STATION, SATELLITE 68, 1982

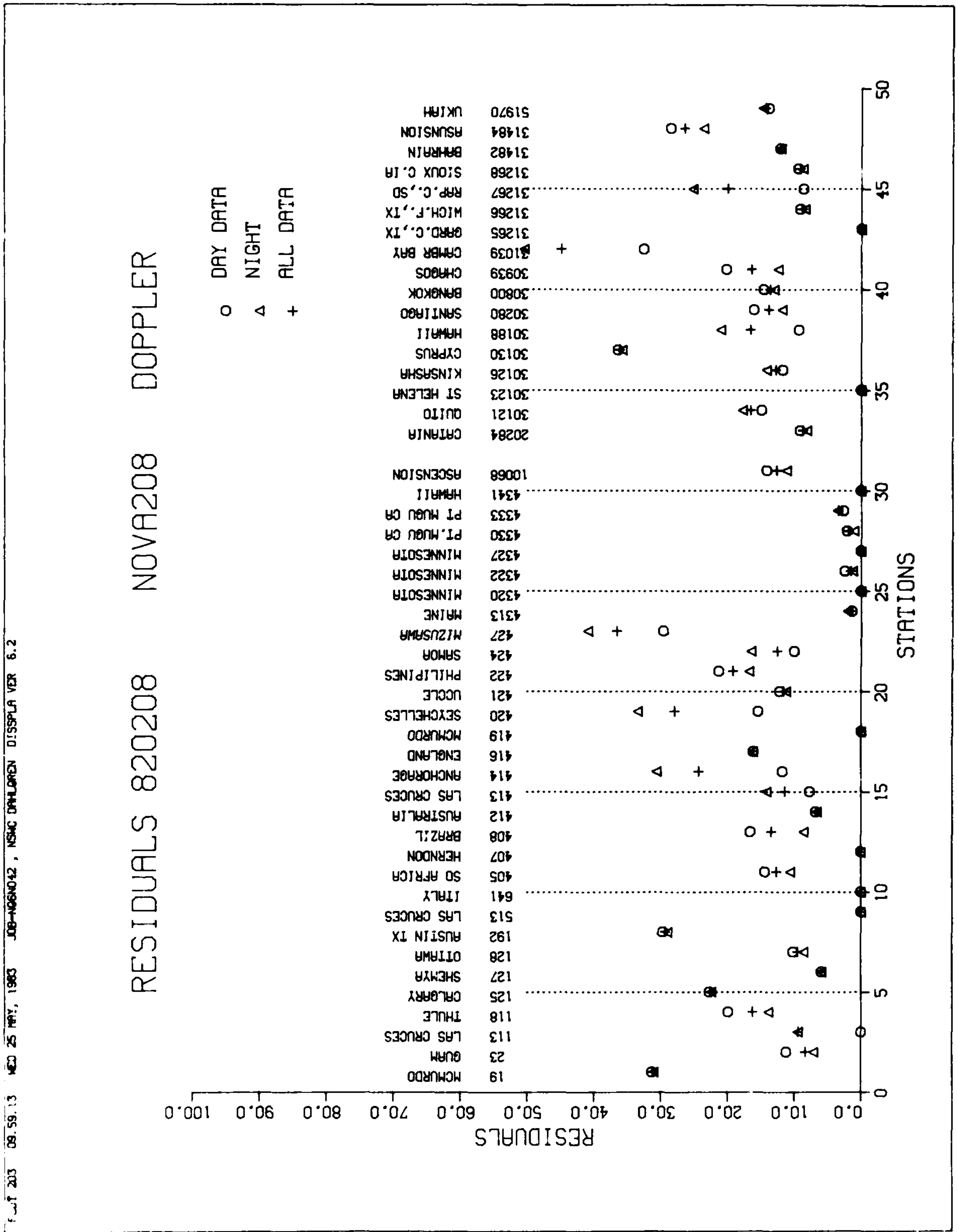

FIGURE A-2d. RESIDUALS BY STATION, NOVA, 1982

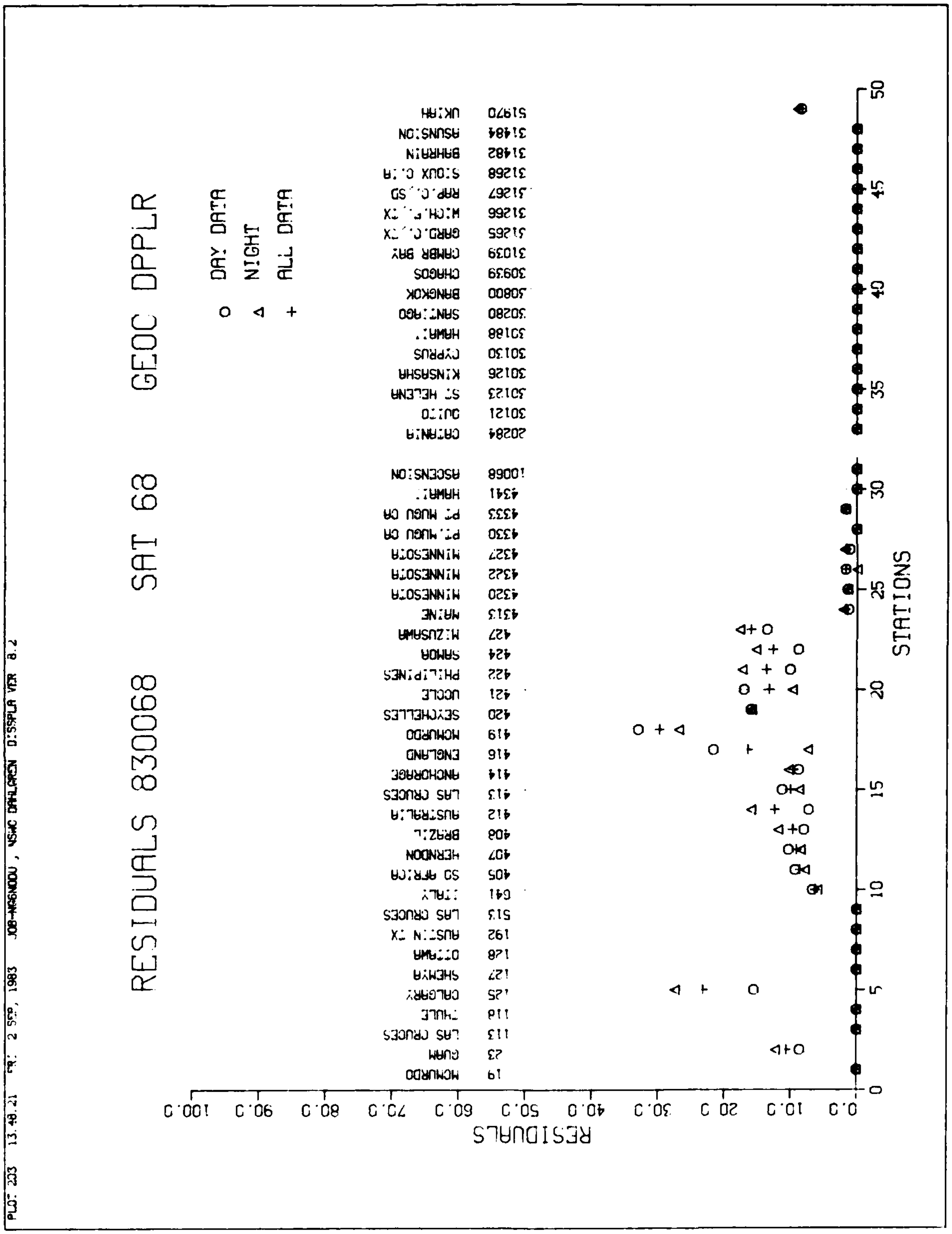

FIGURE A-2e. RESIDUALS BY STATION, SATELLITE 68, 1983

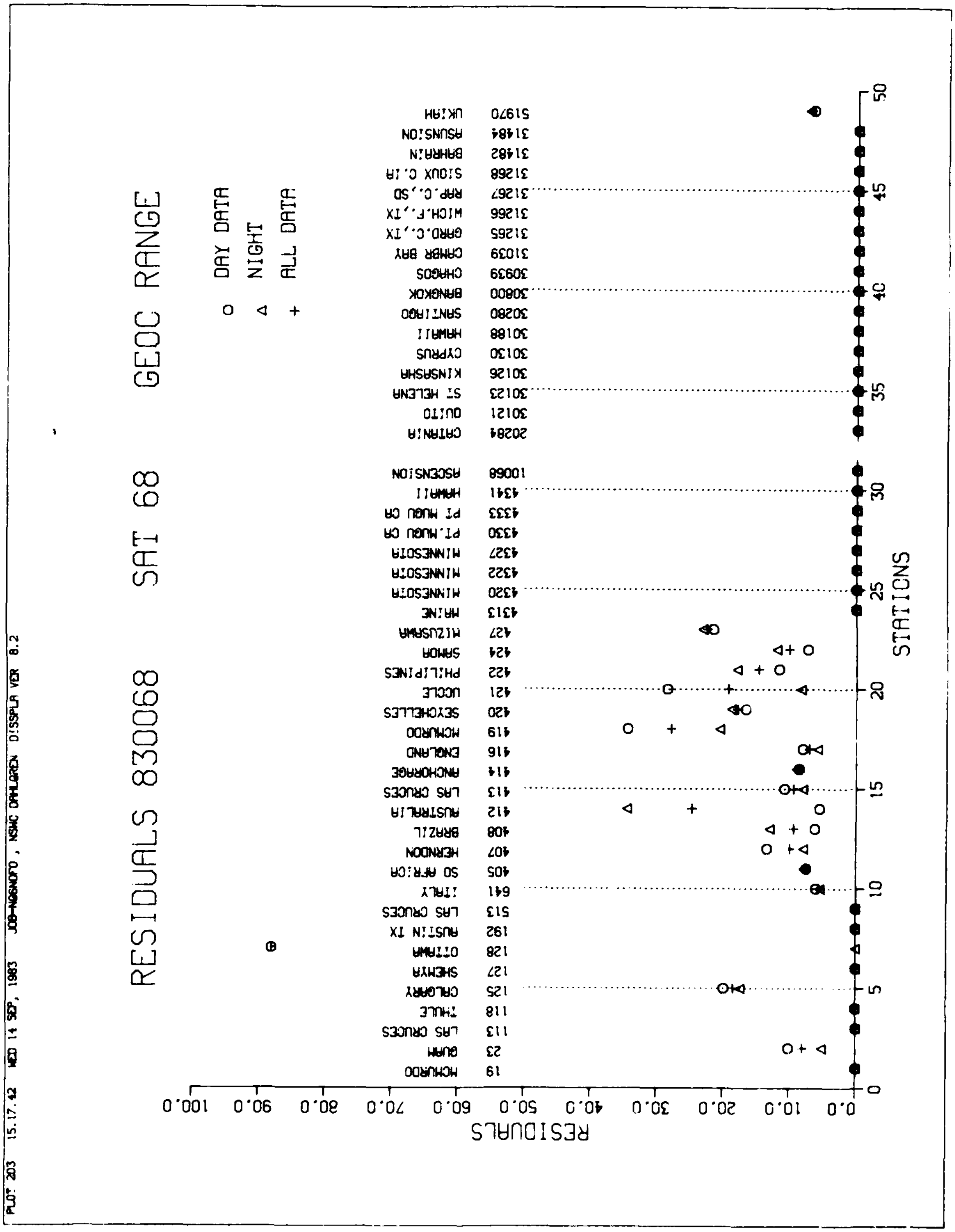

FIGURE A-2f. RESIDUALS BY STATION, SATELLITE 68, 1983, RANGE DATA

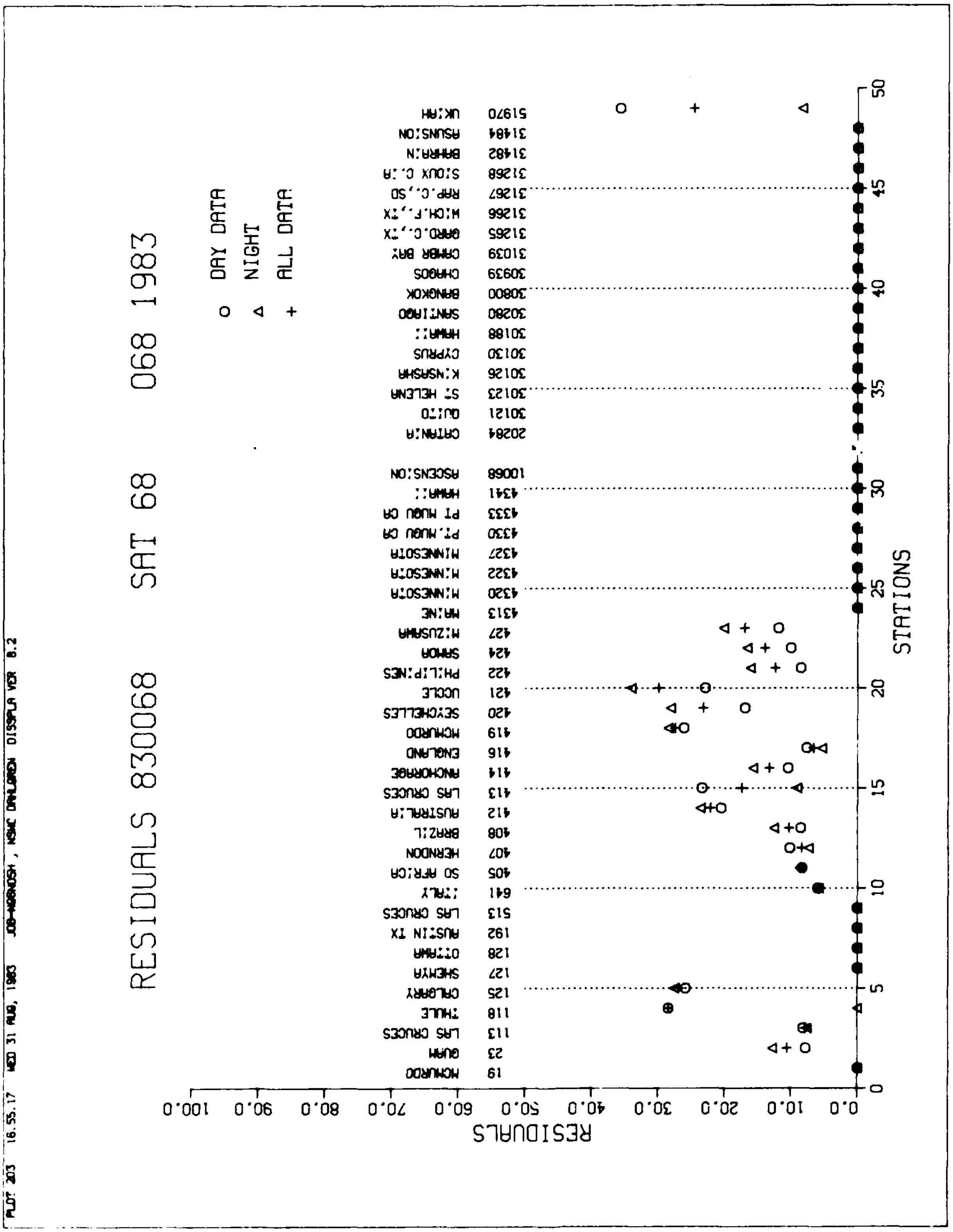

FIGURE A-2g. RESIDUALS BY STATION, SATELLITE 68, 1983, NORMAL PROCESSING

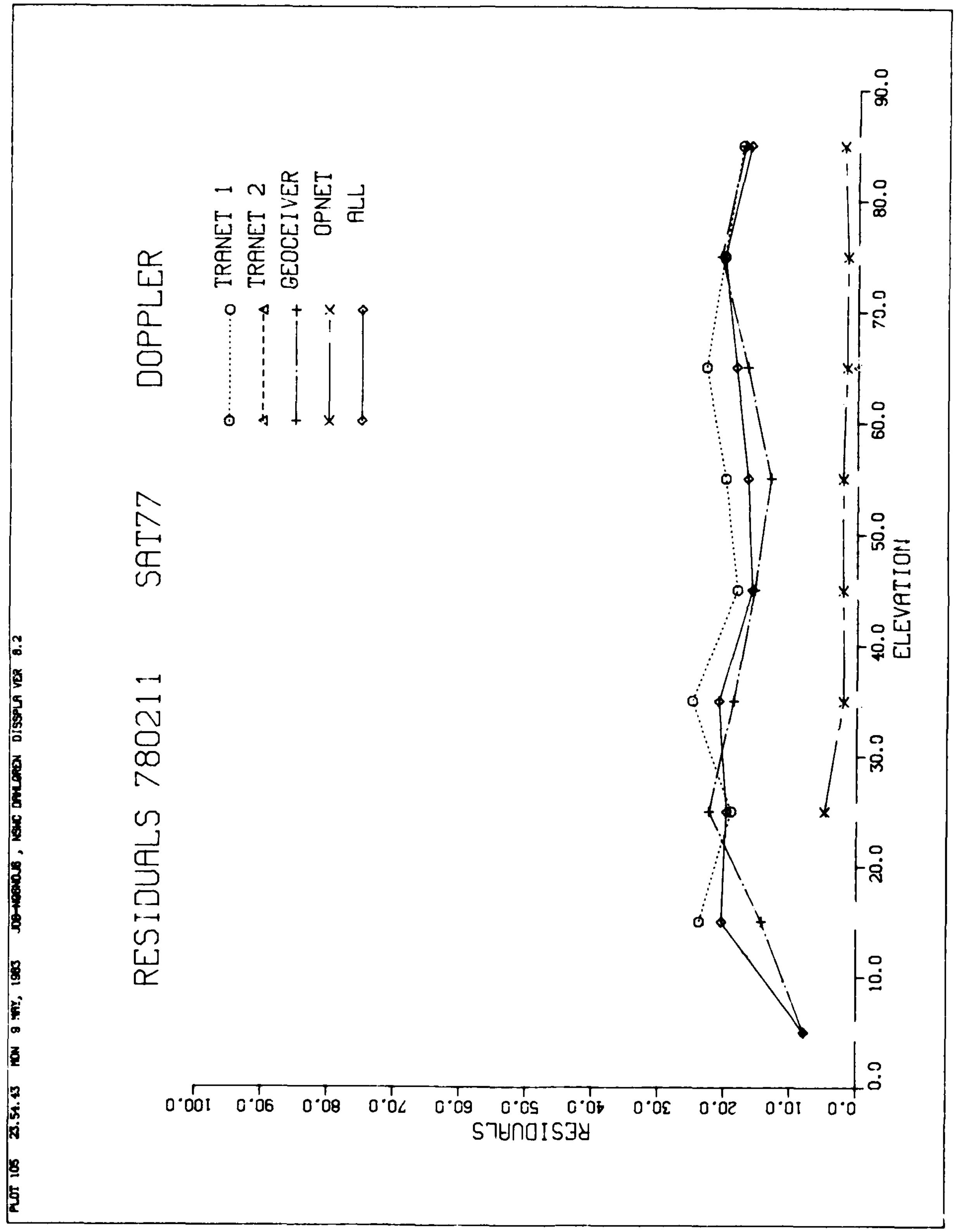

FIGURE A-3a. RESIDUALS BY ELEVATION ANGLE, SATELLITE 77, 1978

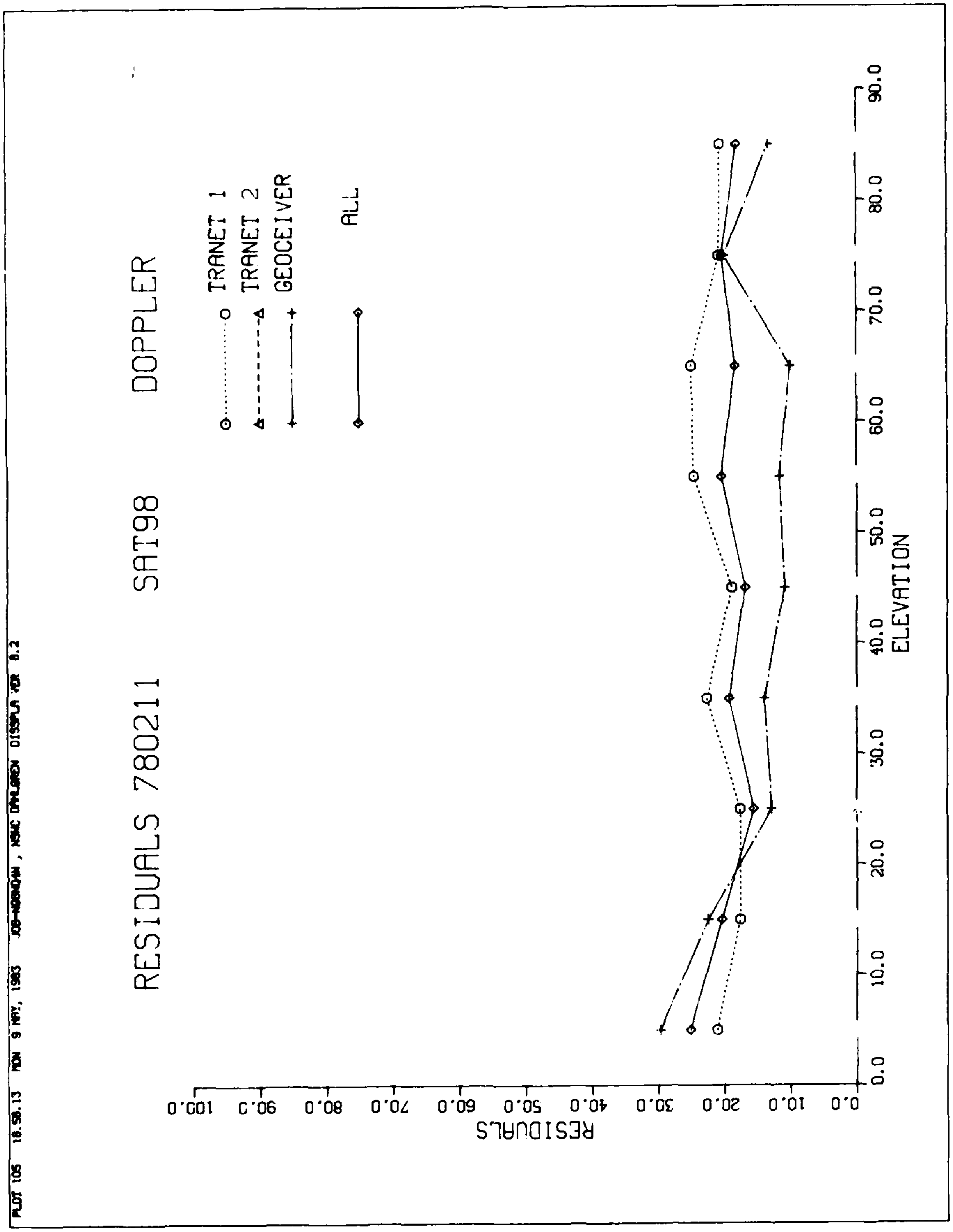

FIGURE A-3b. RESIDUALS BY ELEVATION ANGLE, SATELLITE 98, 1978

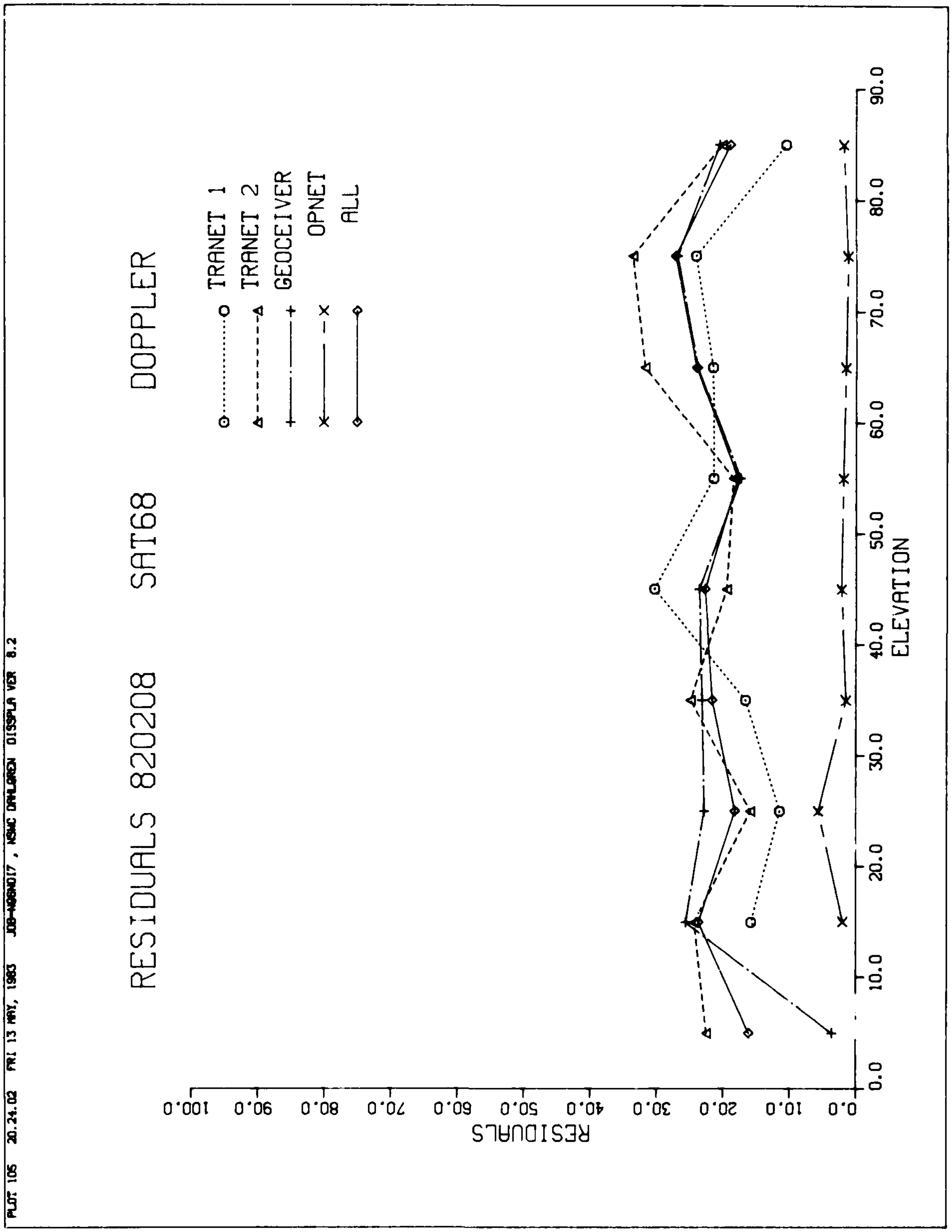

FIGURE A-3c. RESIDUALS BY ELEVATION ANGLE, SATELLITE 68, 1982

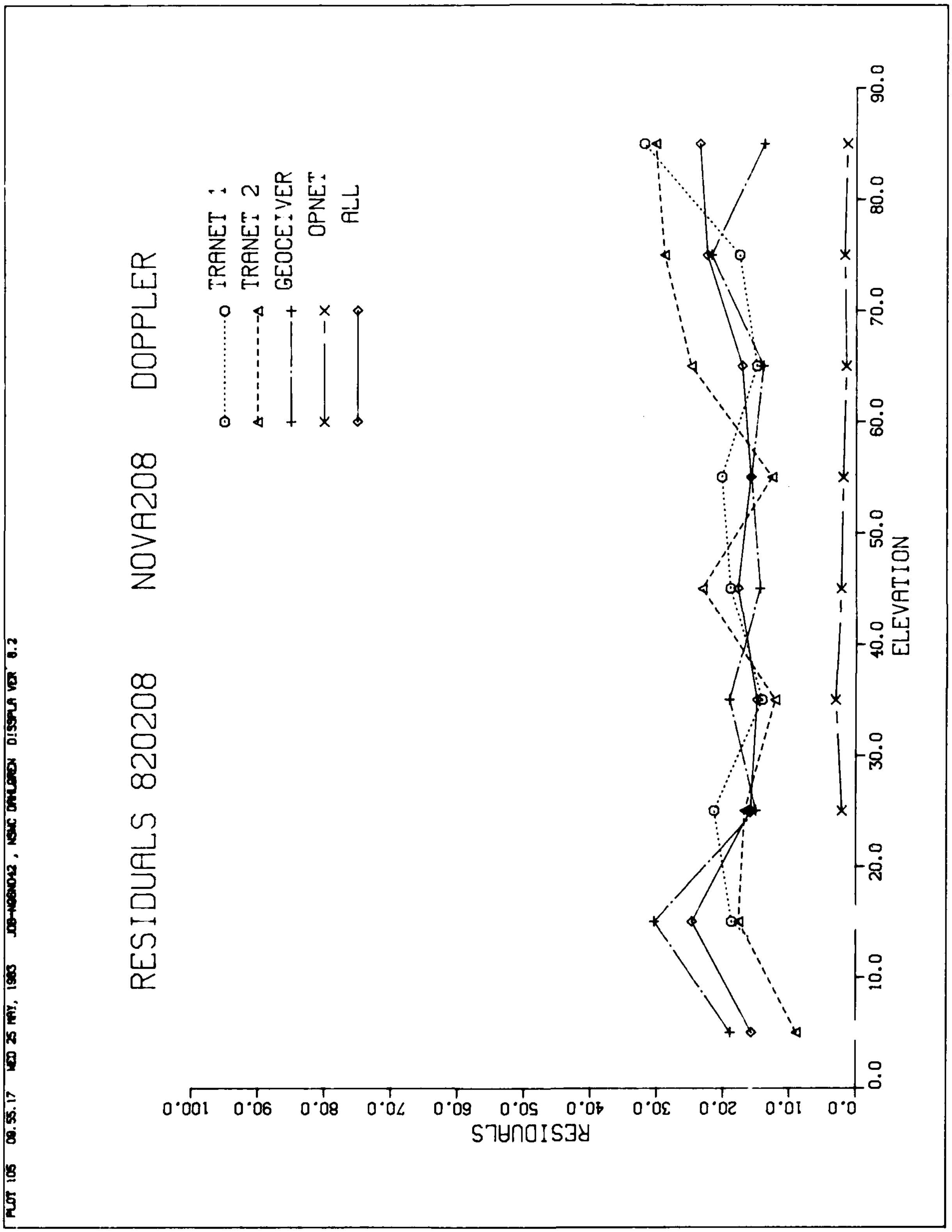

FIGURE A-3d. RESIDUALS BY ELEVATION ANGLE, NOVA, 1982

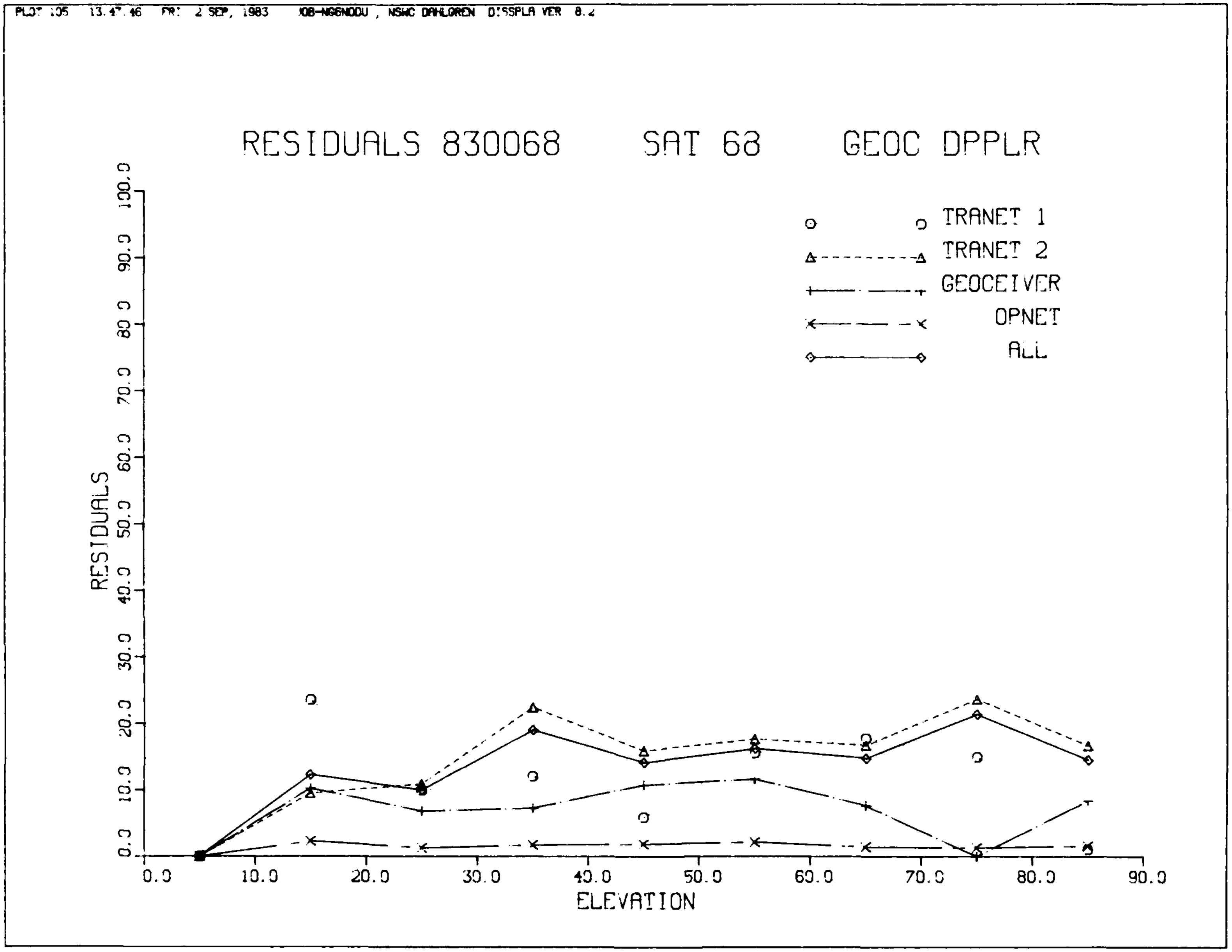

FIGURE A-3e. RESIDUALS BY ELEVATION ANGLE, SATELLITE 68, 1983

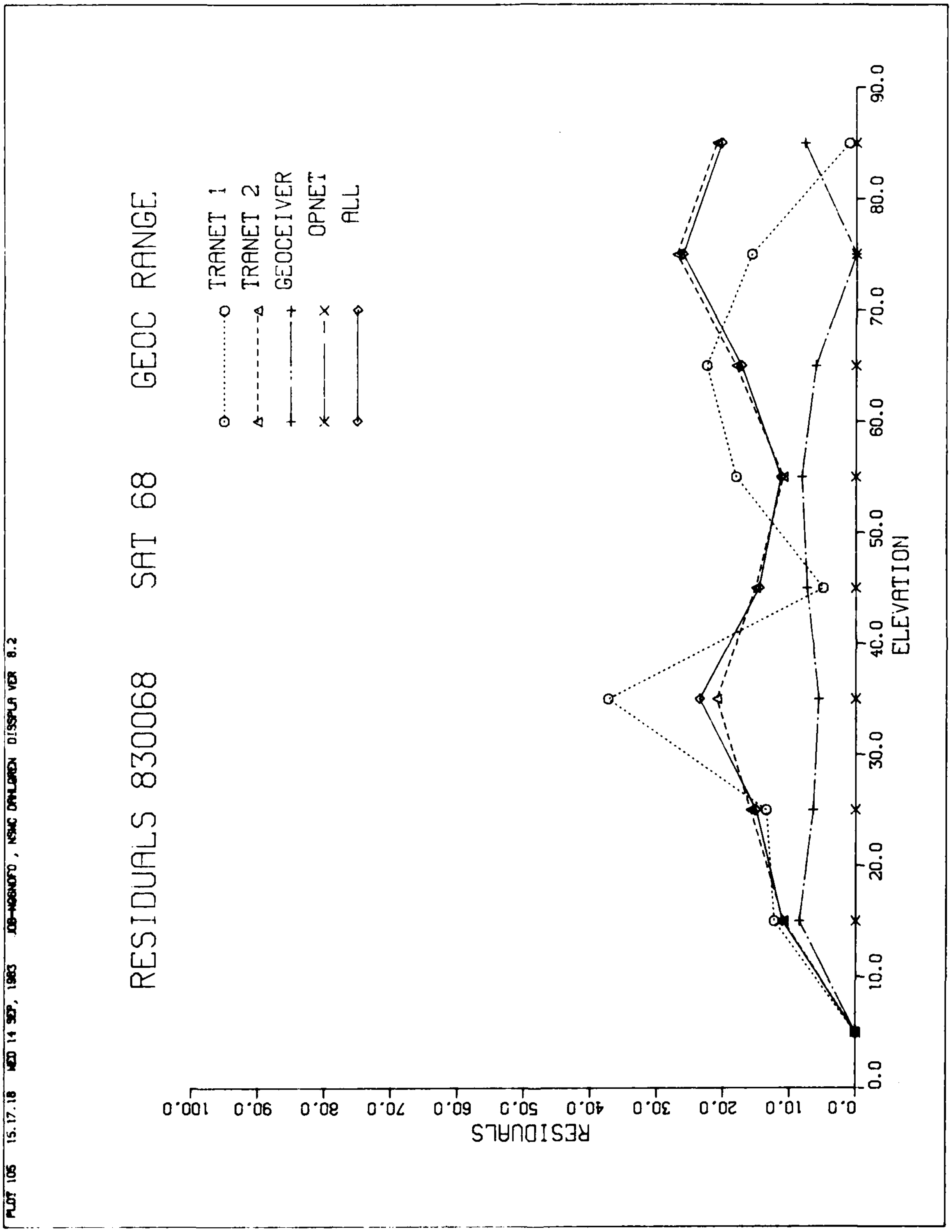

FIGURE A-3f. RESIDUALS BY ELEVATION ANGLE, SATELLITE 68, 1983 RANGE DATA

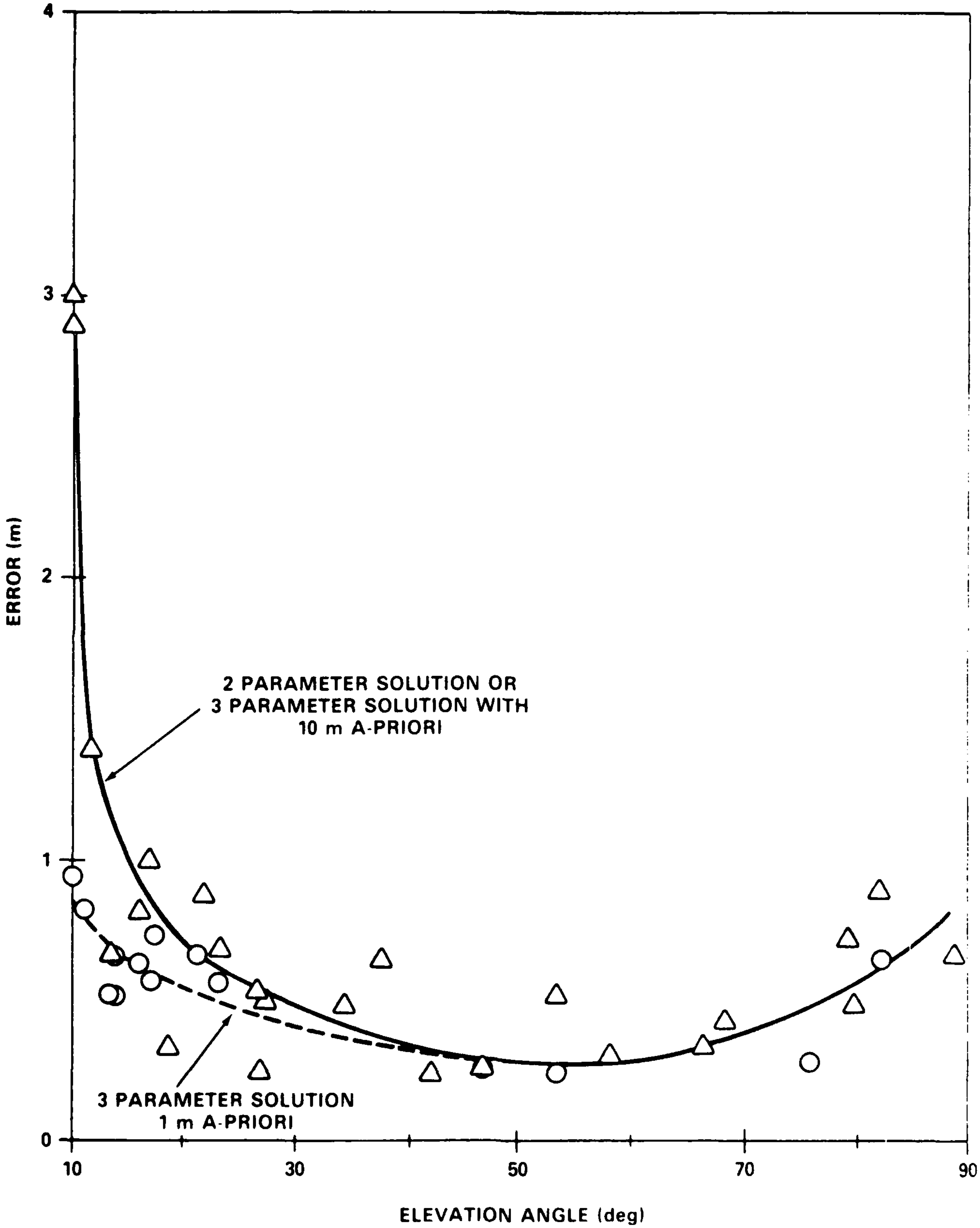

FIGURE A-4a. EFFECT OF PARAMETER SET ON TANGENTIAL STANDARD ERROR

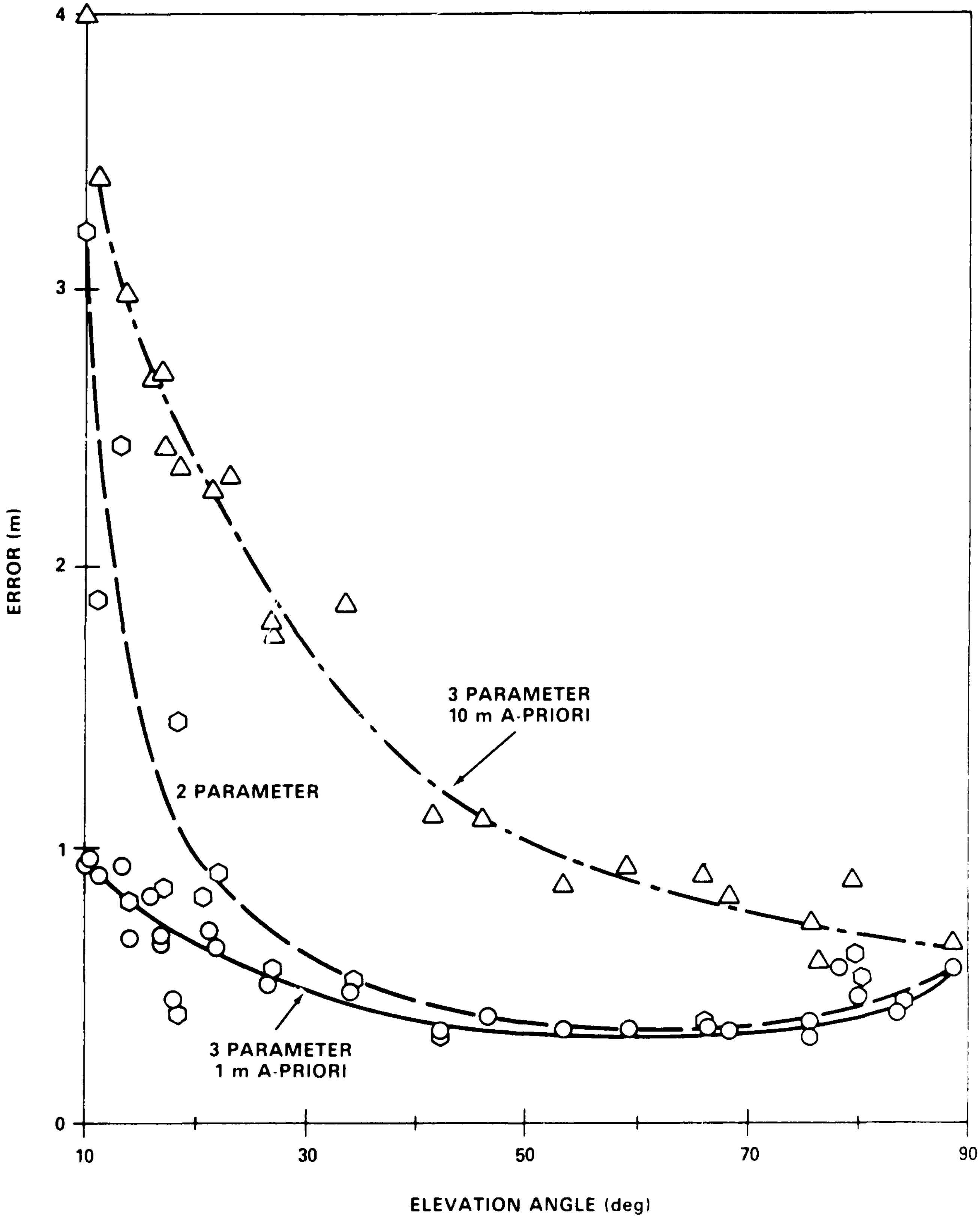

FIGURE A-4b. EFFECT OF PARAMETER SET ON RADIAL STANDARD ERROR

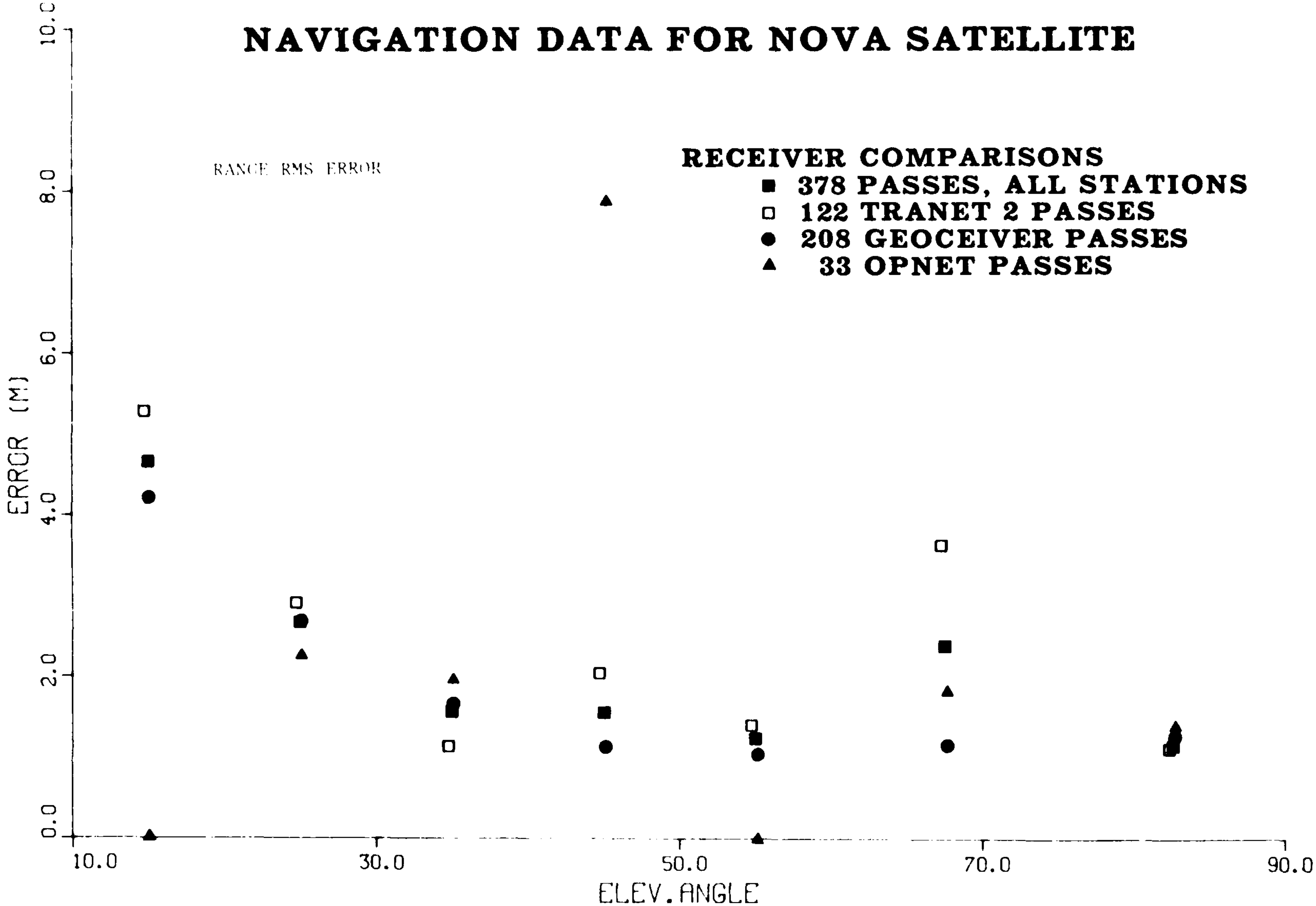

FIGURE A-5a. EFFECT OF EQUIPMENT ON ROOT MEAN SQUARE ERROR IN RANGE

	Copies
Goddard Space Flight Center	
ATTN: Dr. David Smith	1
Mr. James Marsh	1
Dr. Joseph Siry	1
Greenbelt, MD 20771	2
The University of Texas at Austin	
ATTN: Dr. Byron Tapley	1
Austin, TX 78712	2
Applied Research Laboratory	
University of Texas	
ATTN: Dr. Arnold Tucker	1
Dr. George Born	1
Dr. Bob Schutz	1
Austin, TX 78712	4
U.S. Naval Observatory	
ATTN: W. L. Klepczynski	1
D. D. McCarthy	1
Washington, DC 20360	
Massachusetts Institute of Technology	
ATTN: Robert King	
Cambridge, MA 02139	1
Defense Mapping School	
Ft. Belvoir, VA 22060	3
U.S. Navy Astronautics Group	
Point Mugu, CA 93041	2
Pacific Missile Test Center	
Point Mugu, CA 93041	1
Physical Sciences Laboratory	
New Mexico State University	
Box 3 - PSL	
ATTN: Dan Martin	1
Las Cruces, NM 88003	2
Naval Postgraduate School	
ATTN: Prof. Chris Mooers	1
Prof. Joseph VonSchwind	1
CDR D. E. Puccini	1
Monterey, CA 93940	
Dept. of Earth & Space Science	
University of California	
ATTN: Prof. William M. Kaula	1
Los Angeles, CA 90024	

	Copies
Jet Propulsion Laboratory	
ATTN: Dr. William Melbourne, 238-540	
4800 Oak Grove Dr.	
Pasadena, CA 91109	3
The Ohio State University	
Dept. of Geodetic Science & Surveying	
ATTN: Dr. Richard Rapp	1
Dr. Ivan Mueller	1
Dr. Urho Uotila	1
1958 Neil Ave.	
Columbus, OH 43210	
Institute for Laboratory Astrophysics	
University of Colorado	
ATTN: Dr. Peter Bender	1
Boulder, CO 80309	
Department of Astronomy	
University of Texas	
ATTN: P. J. Shelus	1
Austin, TX 78712	
U.S. Army Engineers	
Topographic Laboratory	
Ft. Belvoir, VA 22060	1
DMA-IAGS Cartographic School	
P.O. Drawer 934, Fort Clayton	
APO Miami, FL 34004	5
Naval Space Surveillance System	
Dahlgren, VA 22448	1
Headquarters Space Division (AFSC)	
Los Angeles Air Force Station	
Box 92960 Worldway Postal Center	
Los Angeles, CA 90009	1
Applied Physics Laboratory	
Johns Hopkins University	
ATTN: Harold Black	1
Vincent Pisacane	1
Johns Hopkins Road	
Laurel, MD 20810	1
Internal Distribution:	
E31 (GIDEP)	1
E411	1
E431	9
F14	4

DISTRIBUTION

	Copies
Defense Mapping Agency Washington, DC 20305	3
Defense Mapping Agency Hydrographic/Topographic Center ATTN: Mrs. Caroline Leroy Washington, DC 20315	10
Defense Mapping Agency Aerospace Center ATTN: Dr. Robert Ballew 3200 South Second Street St. Louis, MO 63118	8
Office of Chief of Naval Operations Naval Oceanography Division (NOP-952) Bldg. 1, U. S. Naval Observatory Washington, DC 20390	2
Naval Oceanographic Office Bay St. Louis, MS 39522	2
Office of Naval Research Physical Sciences Division 800 N. Quincy St. Arlington, VA 22217	2
National Oceanic and Atmospheric Administration National Ocean Survey ATTN: Dr. John Bossler	1
Dr. William Strange	1
Mr. Larry Hothem	1
Rockville, MD 20850	2
Library of Congress ATTN: Gift and Exchange Division Washington, DC 20540	4

	Copies
National Aeronautics and Space Administration Scientific and Technical Library Code NHS 22, Rm. BA39 600 Independence Ave., SW Washington, DC 20546	2
Naval Space Command Dahlgren, VA 22448	1
Naval Electronics Systems Command Navy Space Project, PME106 Washington, DC 20360	3
Office of Naval Operations Navy Space Systems Division (NOP-943) Washington, DC 20350	2
Naval Research Laboratory ATTN: Mr. Al Bartholomew	1
Dr. Peter Vogt	1
Washington, DC 20375	2
Air Force Geophysics Laboratory Hanscom Field Bedford, MA 01731	2
U.S. Geological Survey ATTN: Paul Needham Reston, VA 22091	2
National Aeronautics and Space Administration ATTN: ERG-2 Washington, DC 20546	3

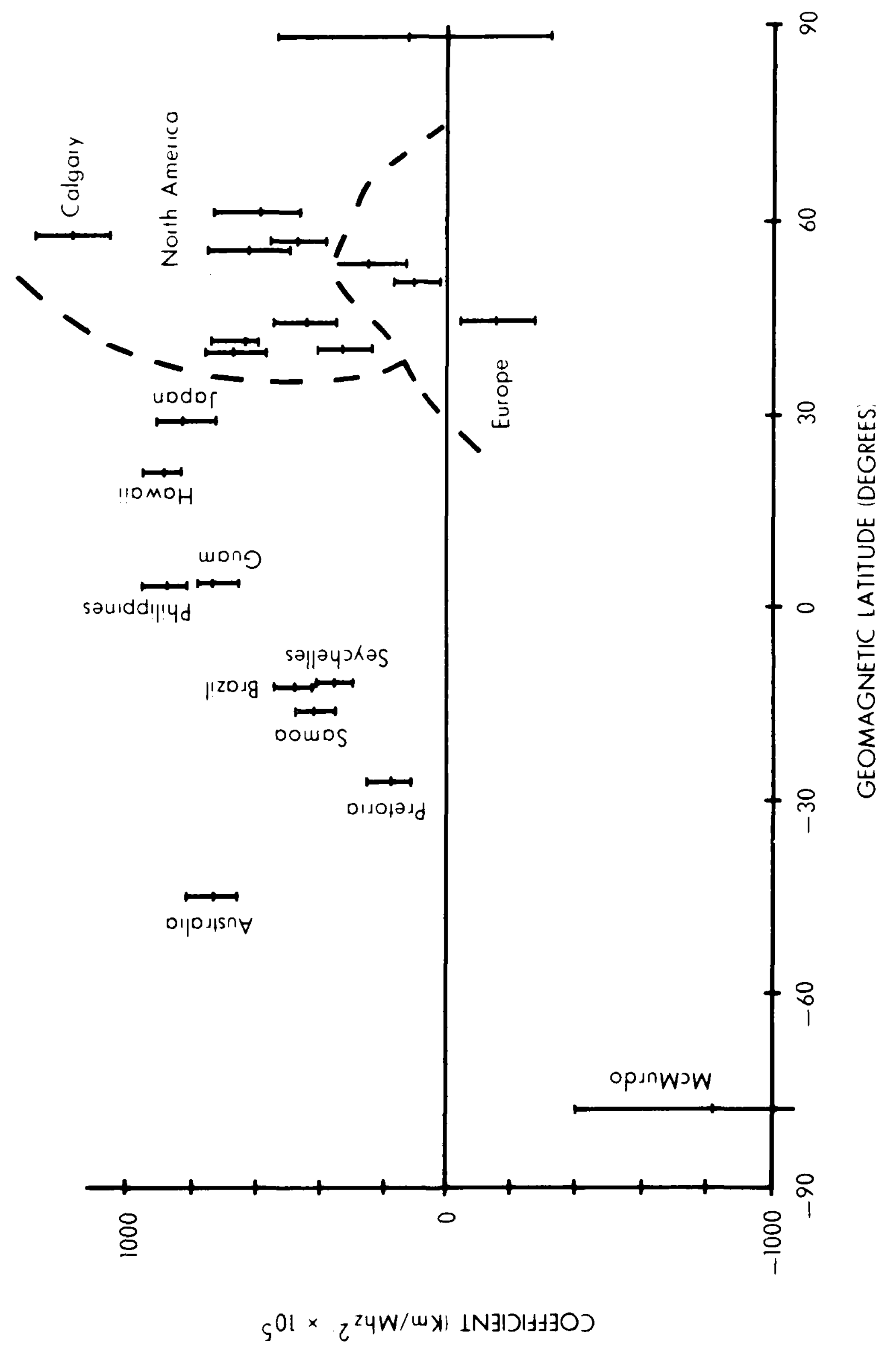

FIGURE A-12. OBSERVED CORRELATION OF CRITICAL FREQUENCY WITH COMPUTED HEIGHT VARIATIONS

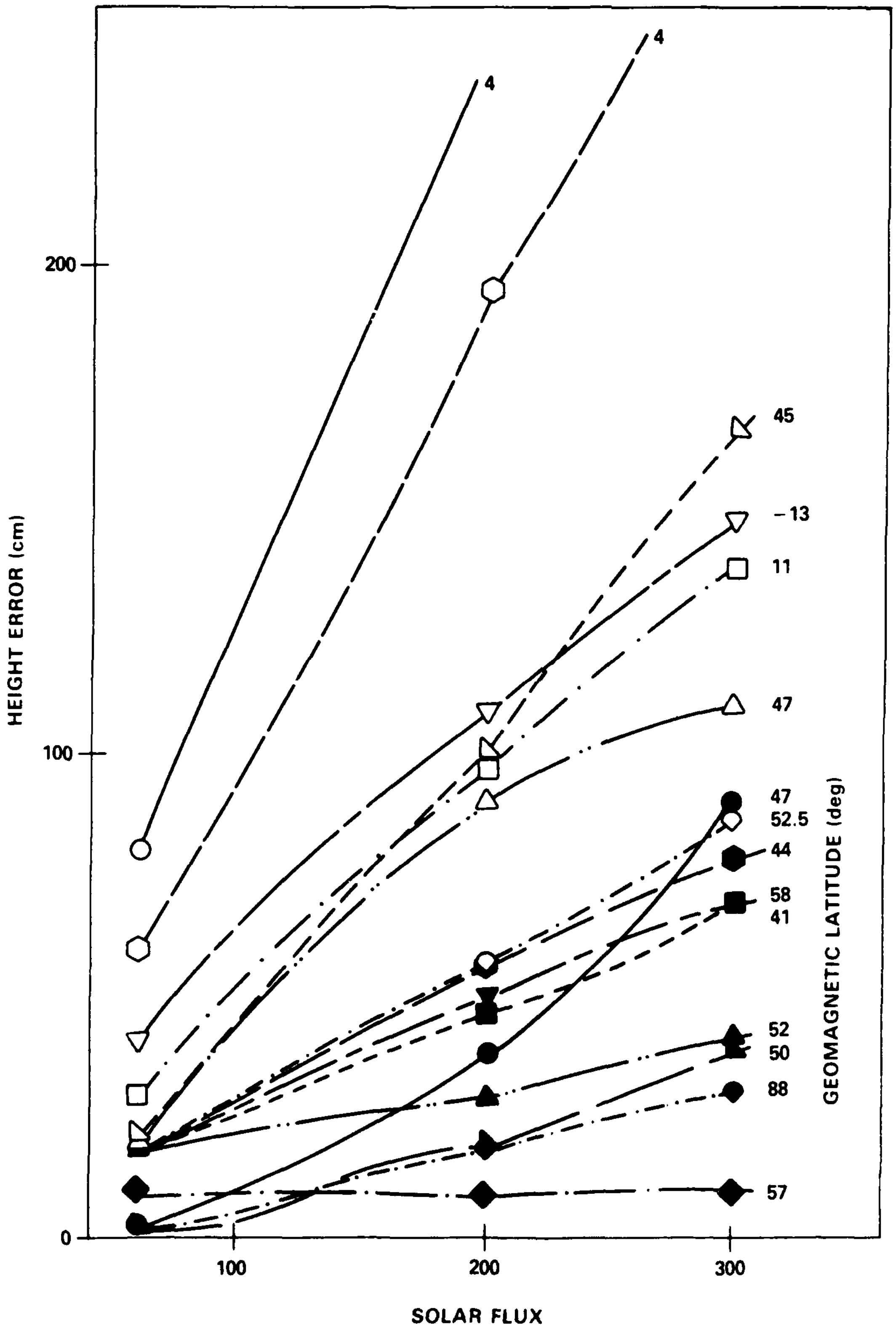

FIGURE A-11. SIMULATED THIRD ORDER IONOSPHERIC EFFECT ON HEIGHT VS SOLAR FLUX

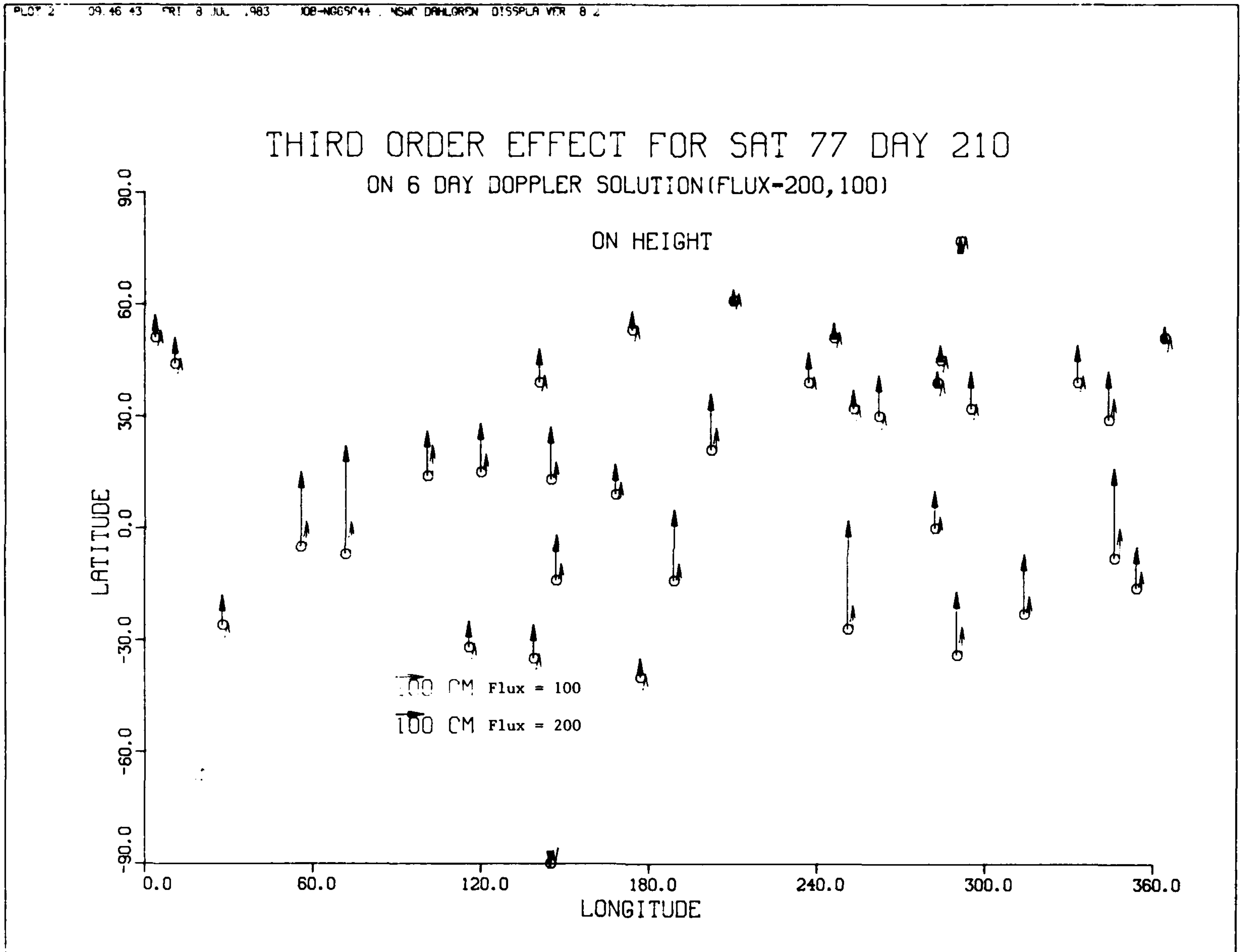

FIGURE A-10b. THIRD ORDER IONOSPHERIC EFFECT ON COMPUTED STATION HEIGHT

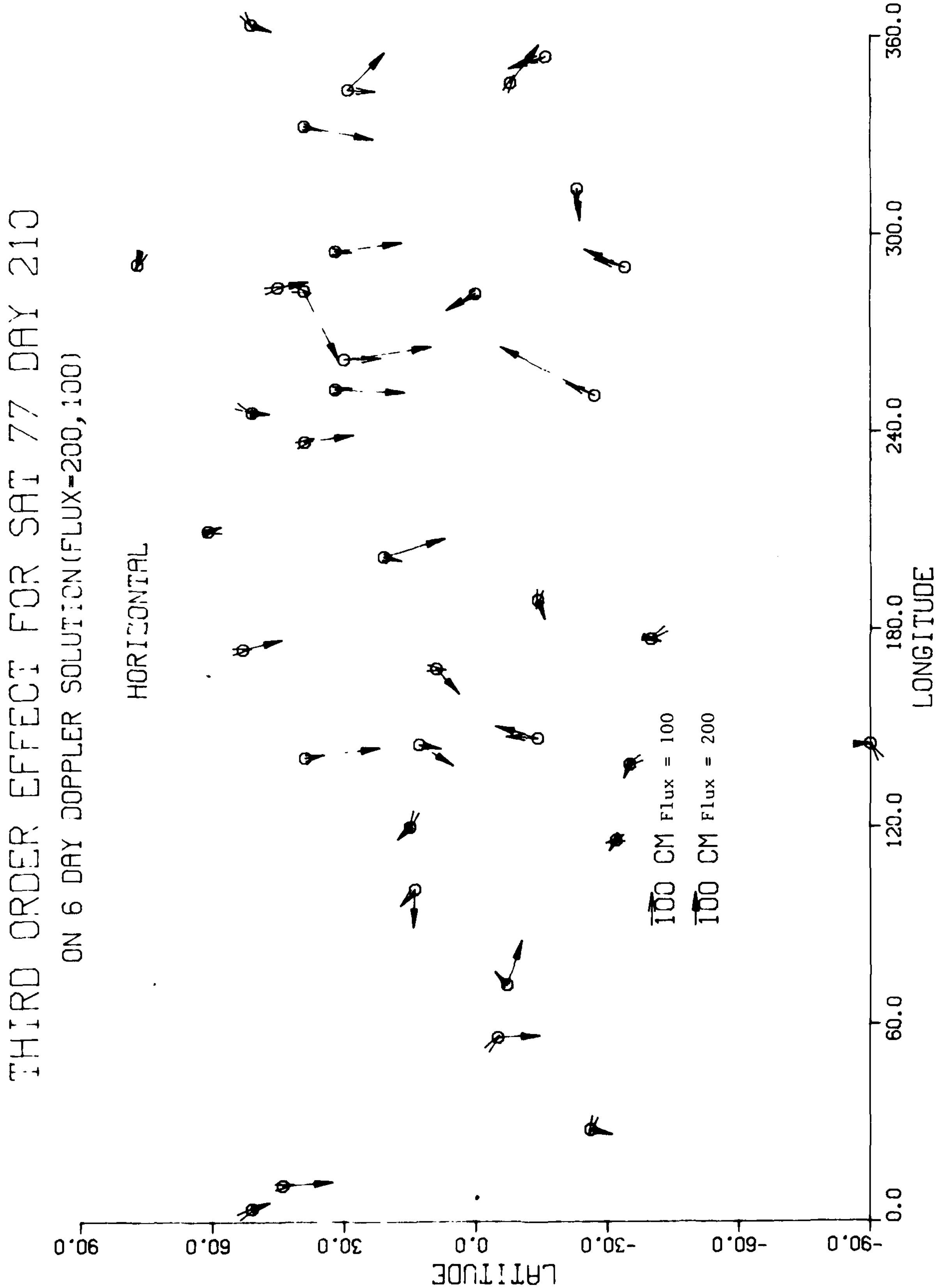

FIGURE A-10a. THIRD ORDER IONOSPHERIC EFFECT ON COMPUTED HORIZONTAL POSITION

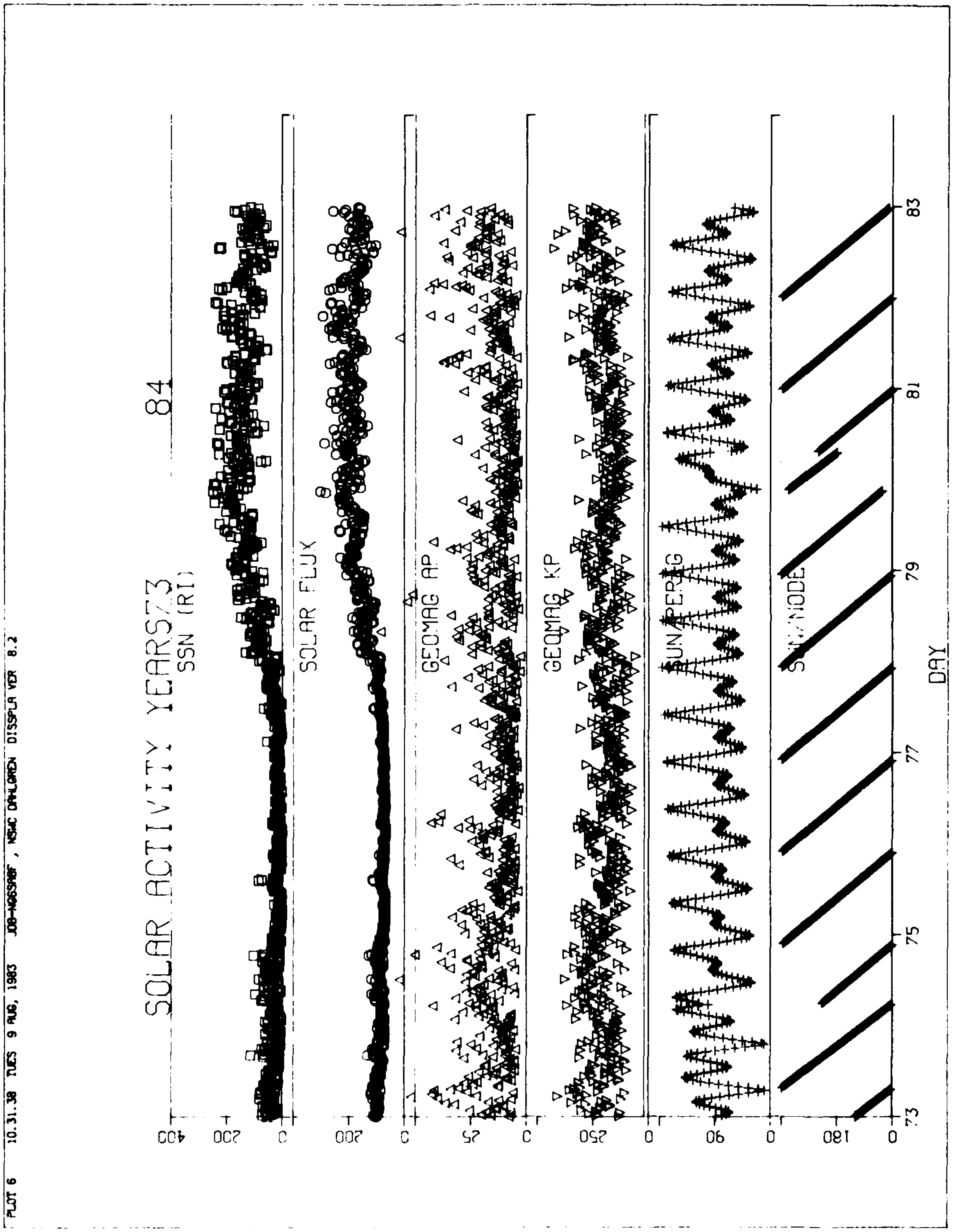

FIGURE A-9. SOLAR ACTIVITY

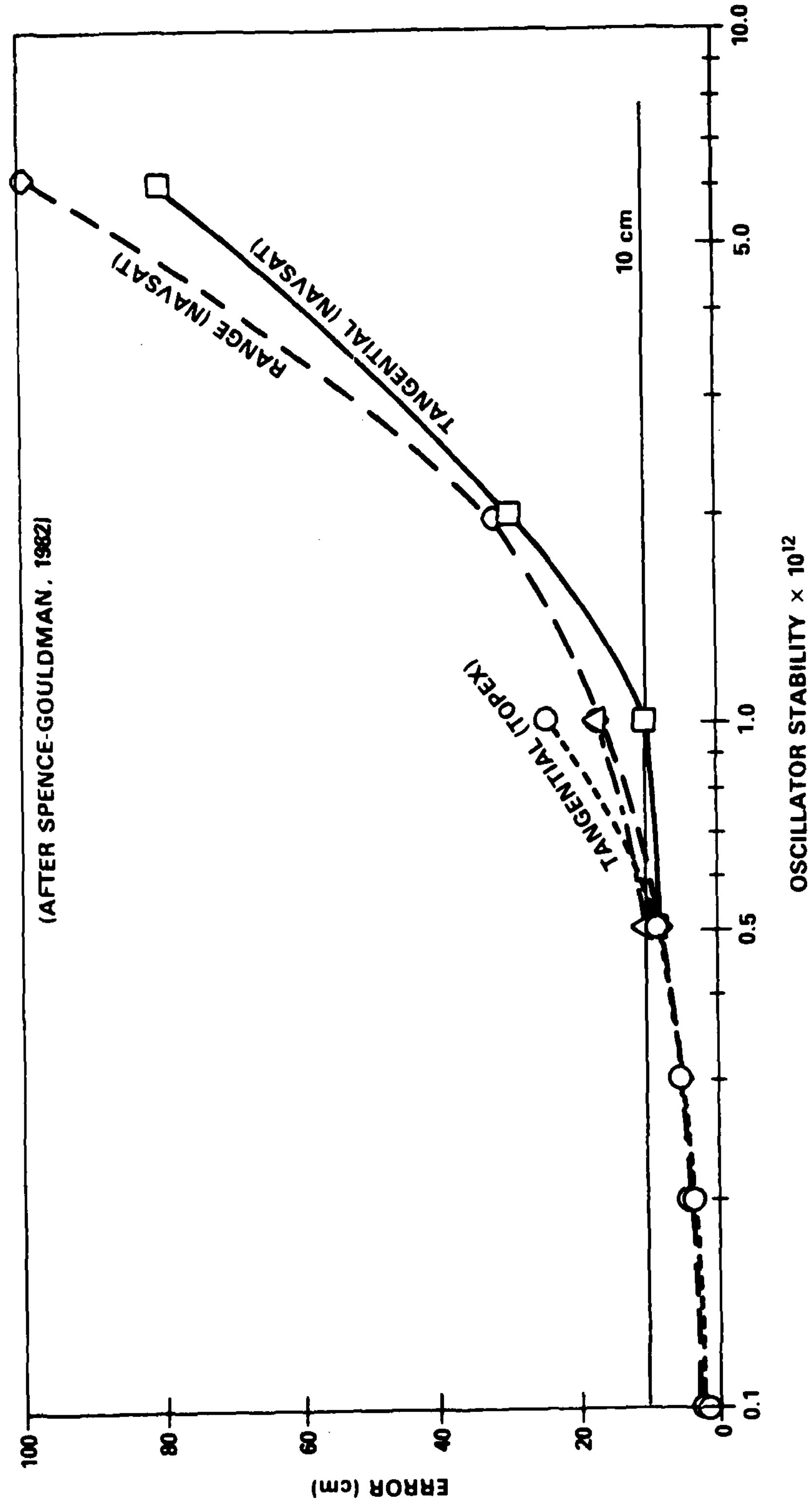

FIGURE A-8. EFFECT OF OSCILLATOR STABILITY ON NAVIGATION ERRORS

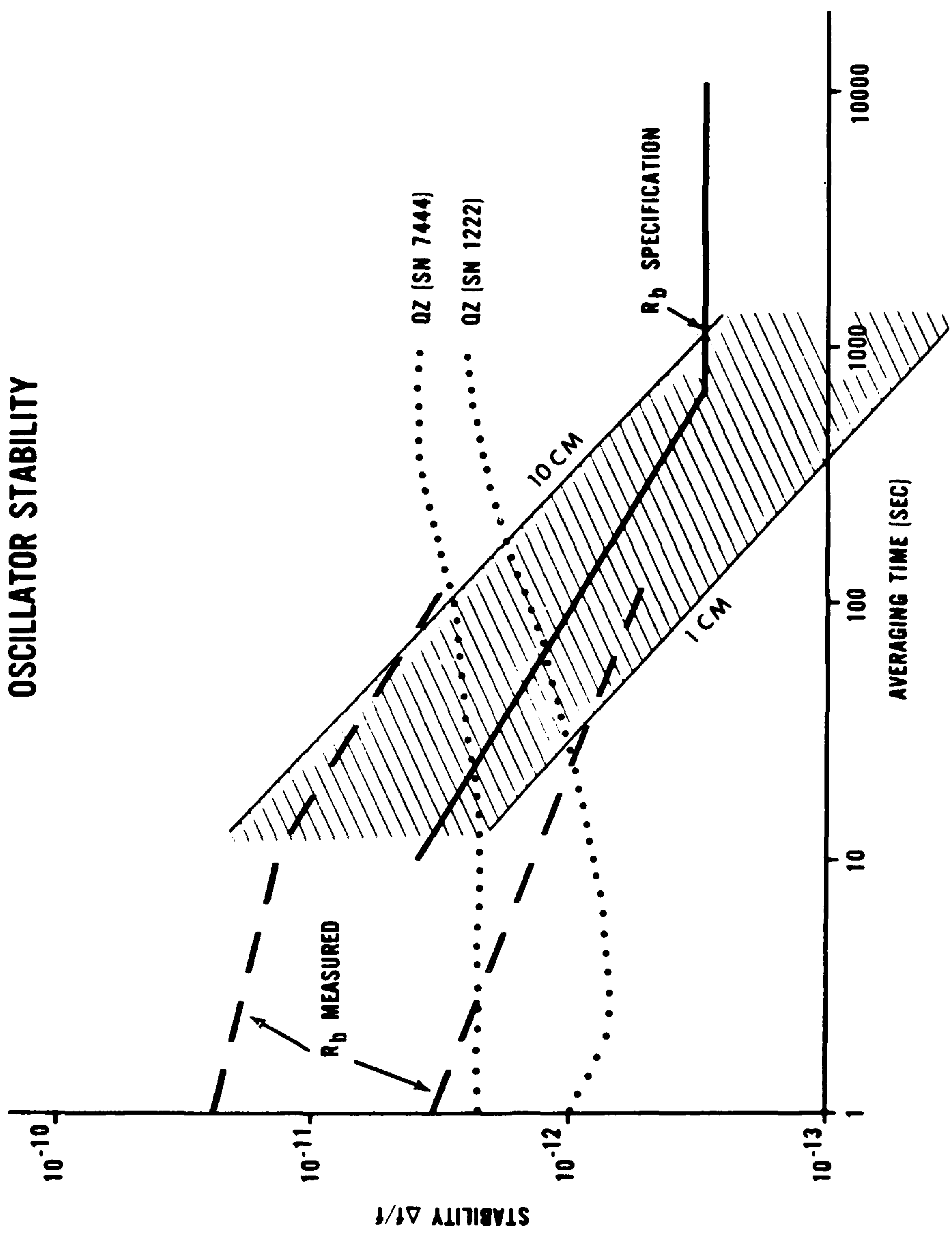

FIGURE A-7. OSCILLATOR STABILITY

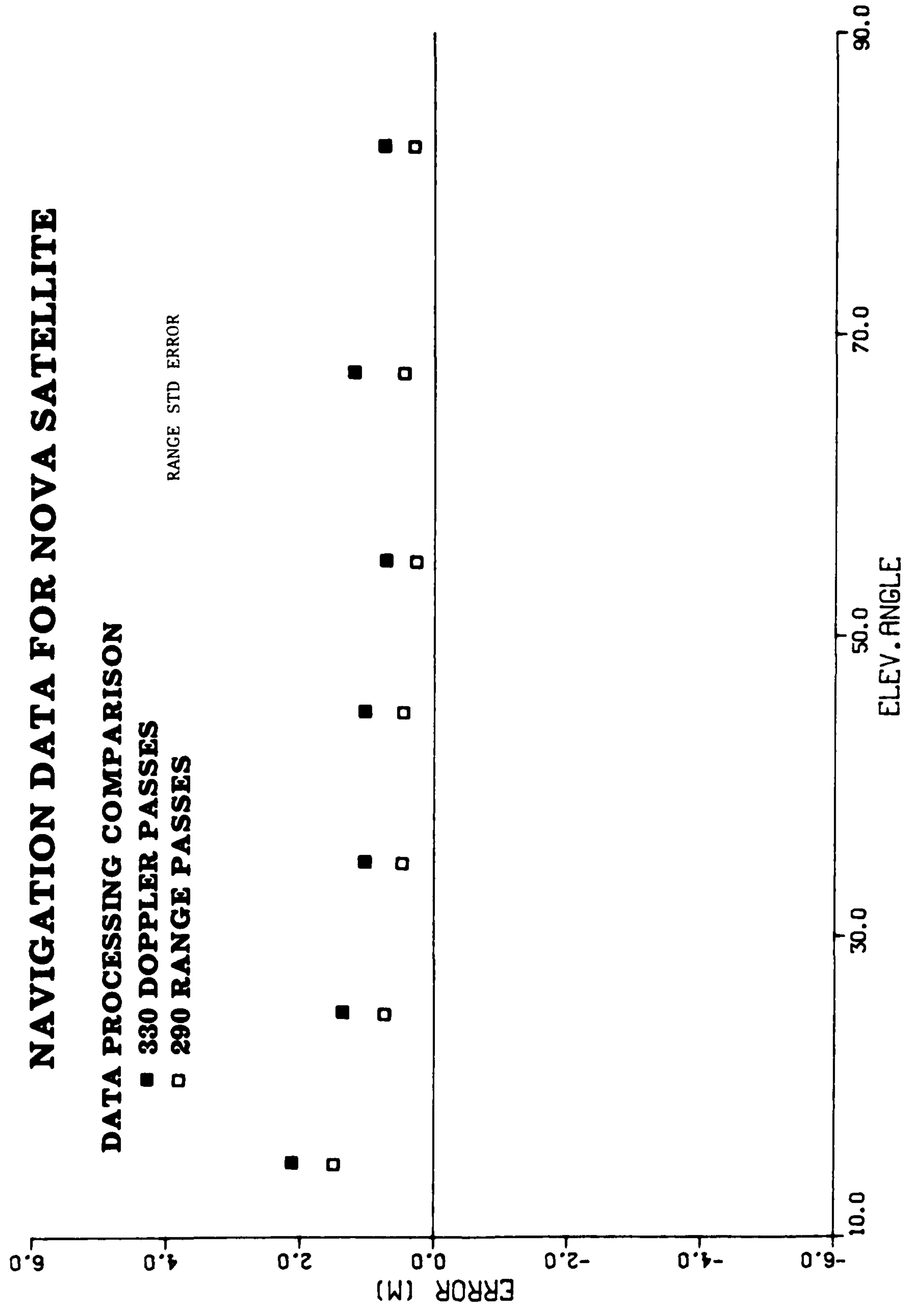

FIGURE A-6c. EFFECT OF DATA PROCESSING ON STANDARD ERROR IN RANGE

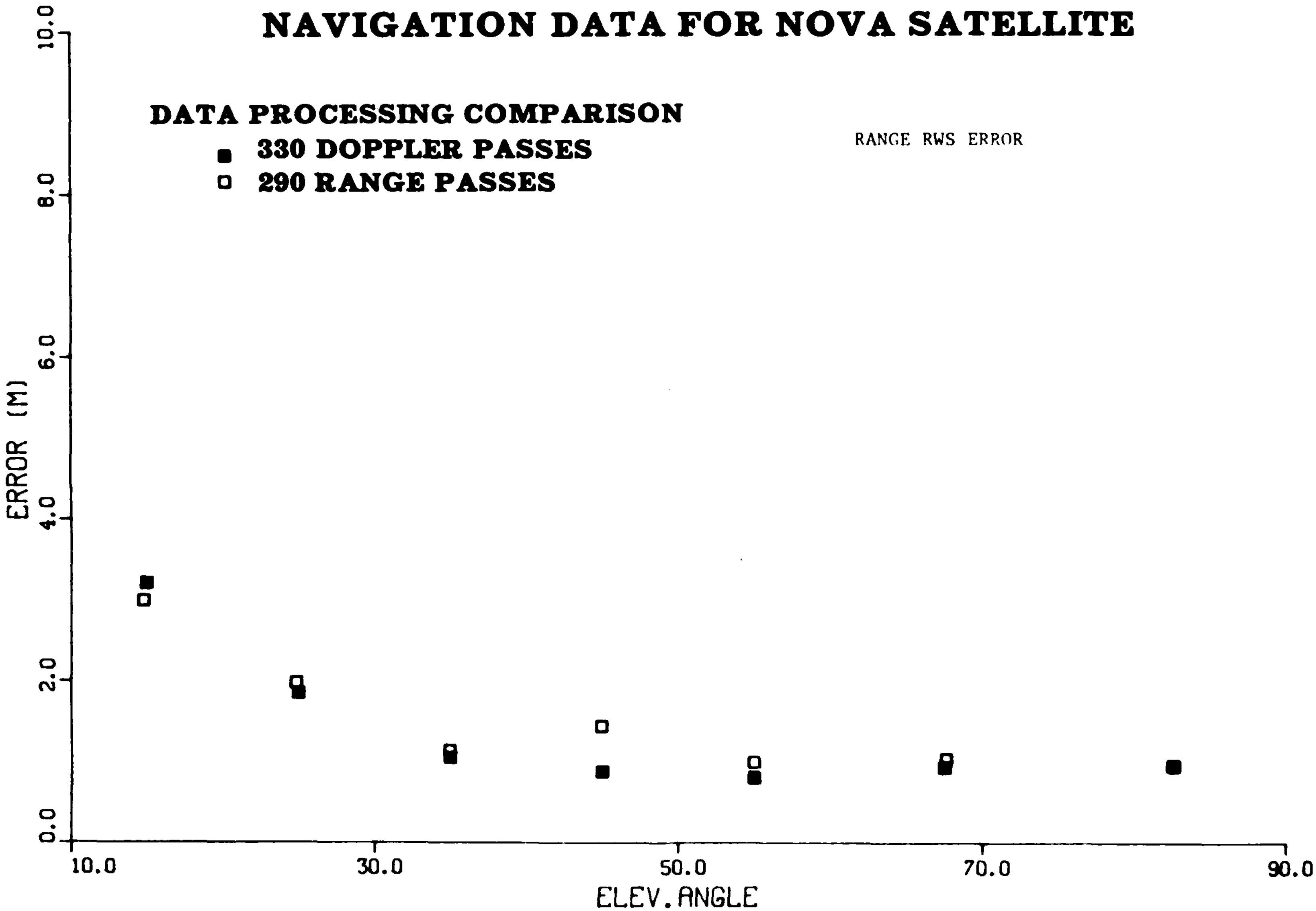

FIGURE A-6b. EFFECT OF DATA PROCESSING ON ROOT WEIGHTED SQUARE ERROR IN RANGE

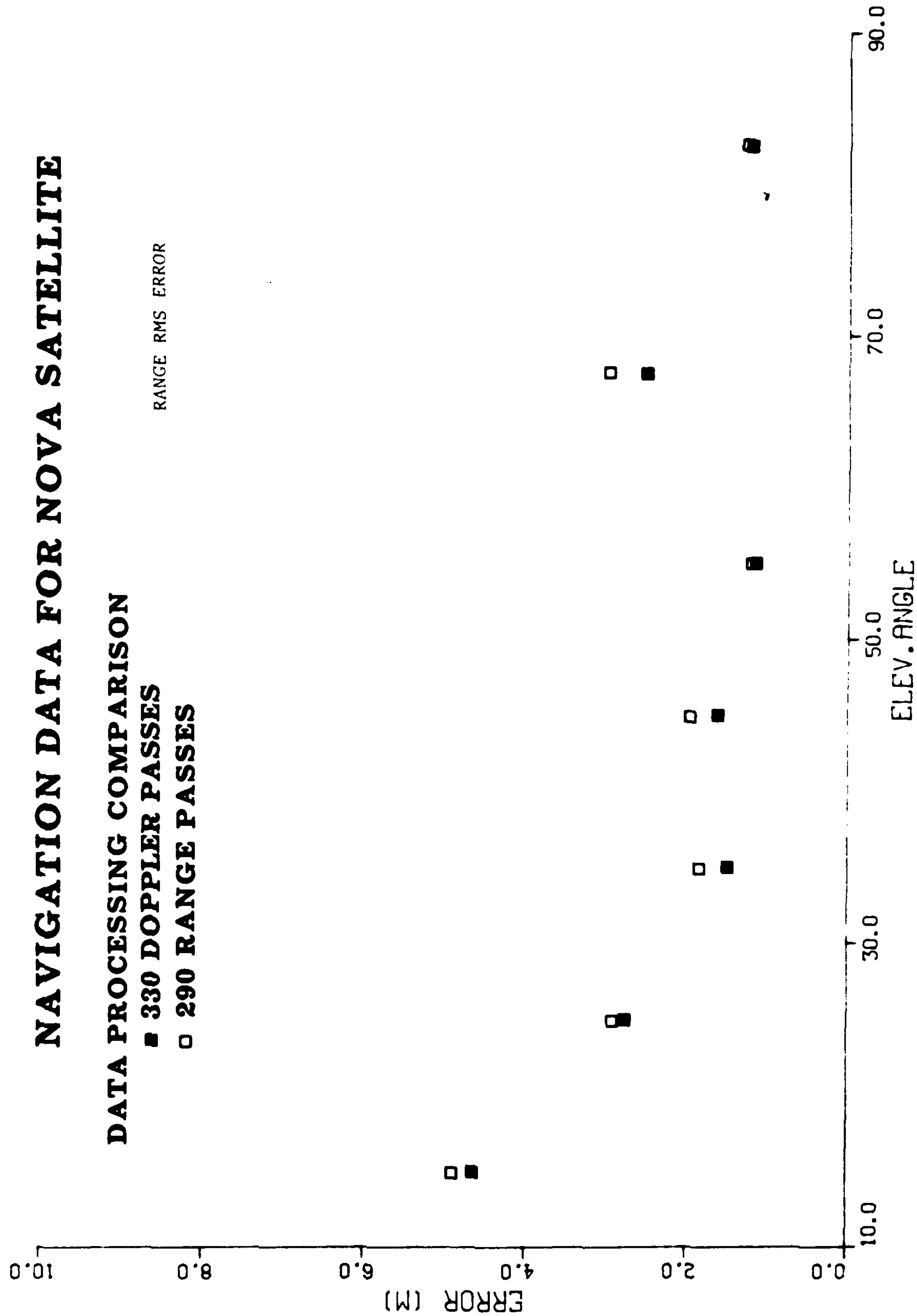

FIGURE A-6a. EFFECT OF DATA PROCESSING ON ROOT MEAN SQUARE ERROR IN RANGE

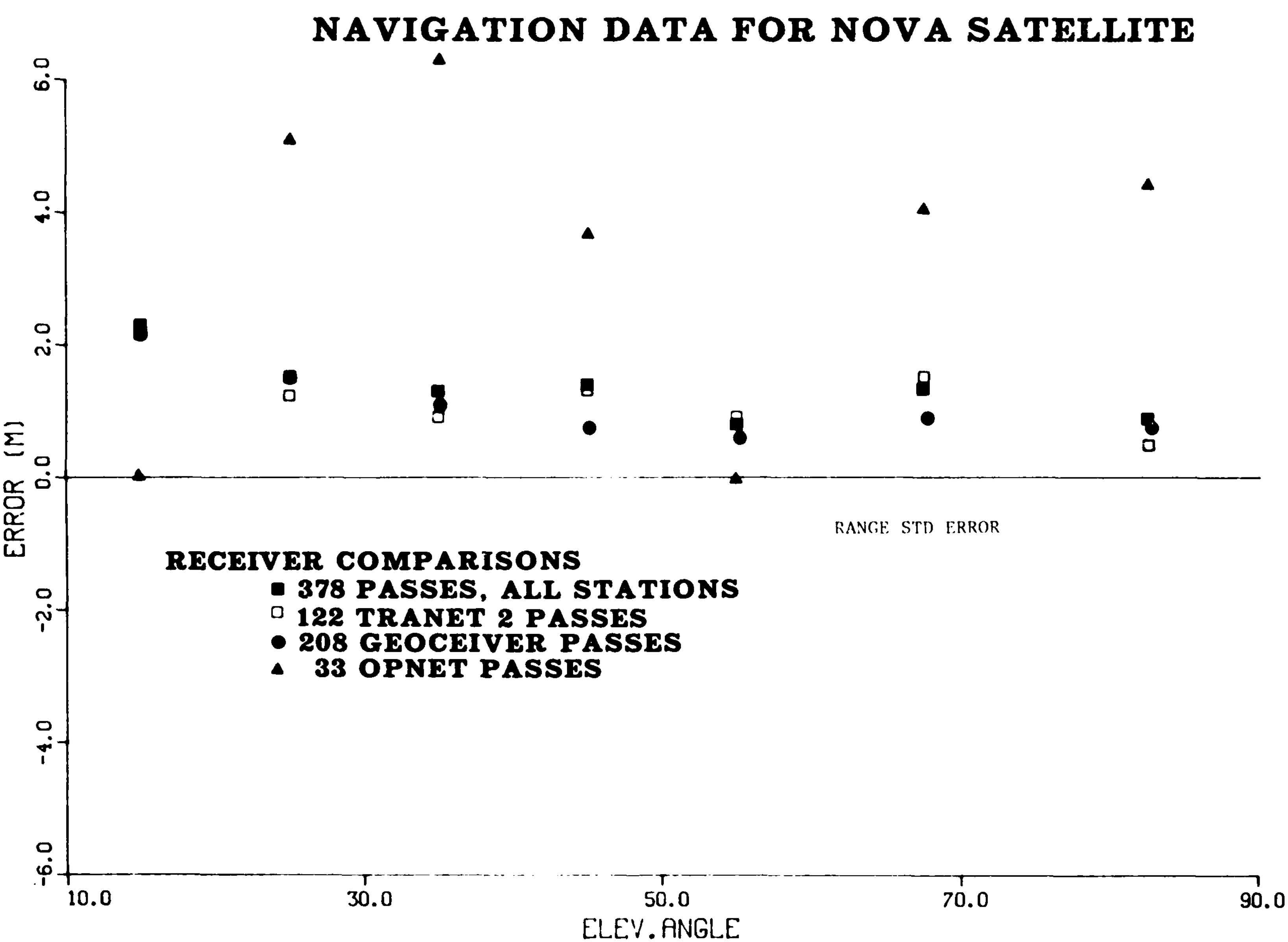

FIGURE A-5c. EFFECT OF EQUIPMENT ON STANDARD ERROR IN RANGE

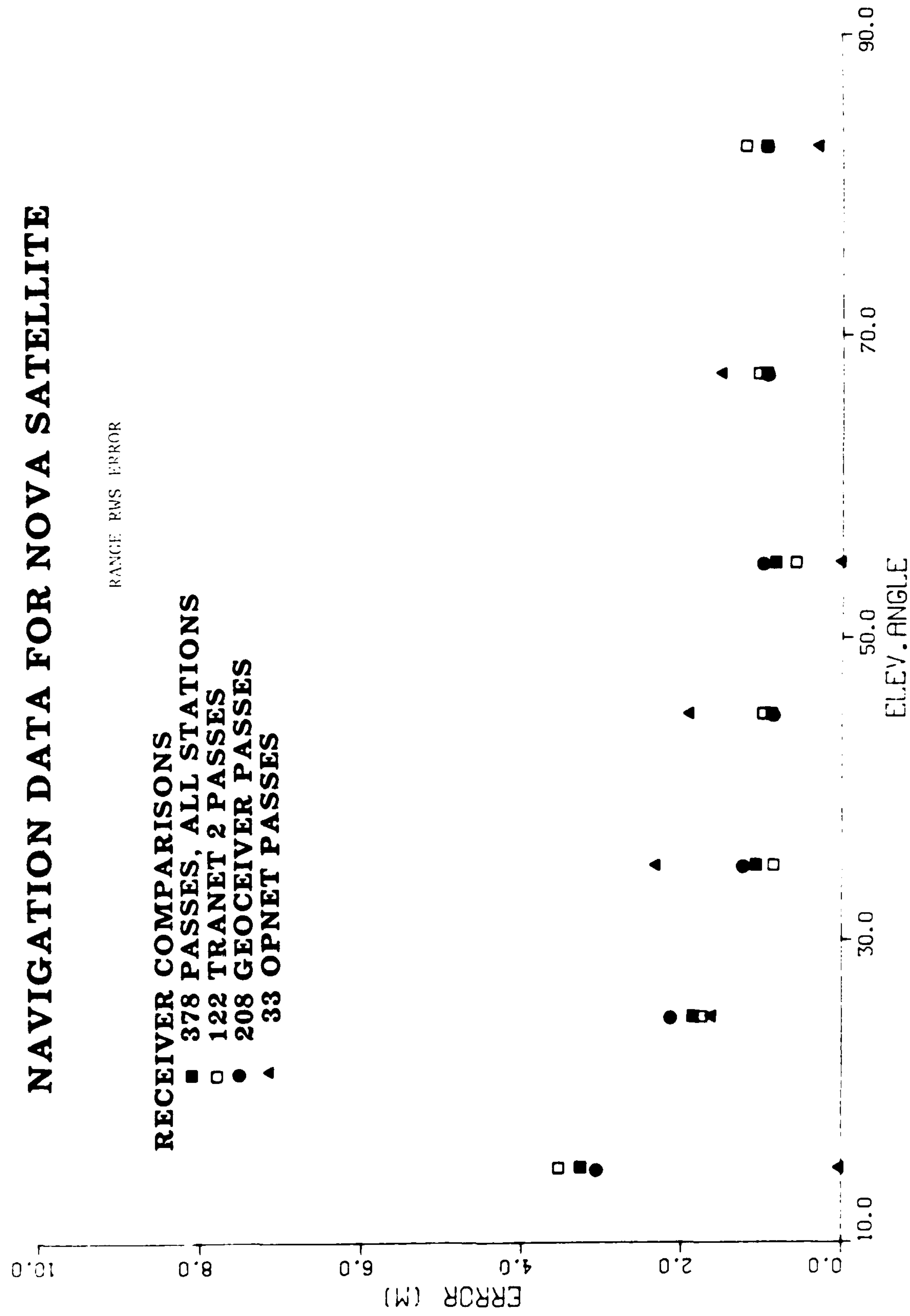

FIGURE A-5b. EFFECT OF EQUIPMENT ON ROOT WEIGHTED SQUARE ERROR IN RANGE

END

FILMED

7-85

DTIC